Interference Cancellation in WCDMA Systems using Tapered Beamformers

A

Thesis

Submitted in the partial fulfillment of requirement for the award of the degree of

Master of Engineering
In
Electronics and Communication

by

Meenakshi Gupta
Regn. No. 8024114

Under the guidance of

Mr. R.K Khanna
Assistant Professor
Department of Electronics &
Communication Engineering

Department of Electronics & Communication Engineering
THAPAR INSTITUTE OF ENGINEERING AND TECHNOLOGY
(Deemed University)
PATIALA-147004

Abstract

The field of wireless communications is growing at an explosive rate, covering many technical areas. The deployment of cellular systems is a success and as the subscriber population continues to grow at a rapid pace, service providers may get capacity problems due to limited available frequency spectrum. Consequently, service providers are forced to find methods of enhancing the coverage and the capacity of their cellular networks. A promising future method suggested is to utilize adaptive antennas, which has also been recognized as one potential economic approach. Adaptive base station antennas have been proposed as a means to achieve the requested longer range and higher capacity in cellular systems.

In WCDMA, there is large number of interferers present in the system due to frequency reuse factor of one. The large numbers of interferers in these systems require a beamforming technique that would efficiently suppress the power in the undesired direction at the same time maximizing the power in the desired direction. For these systems side lobe adjustment would be a simple solution towards suppressing intercell and intracell interference and hence improving CIR performance rather than placing the nulls in the direction of individual interferers.

In this dissertation, a novel two-step tapered beamforming algorithm is analyzed for flexible side lobe adjustment. The algorithm places a very low side lobe level over a large width in the beam pattern. The convergence of this algorithm is fast and requires only two to three iterations. This beamforming algorithm is suitable

for uplink and downlink since it is based on the DOAs estimated in uplink. The algorithm provides flexible parameter adjustment (side lobe level, null depth, main lobe width and null width) together with very low computational effort.

Chapter 1

Introduction

1.1 History of SDMA

The field of wireless communications is growing at an explosive rate, covering many technical areas. The deployment of cellular systems is a success and as the subscriber population continues to grow at a rapid pace, service providers may get capacity problems due to limited available frequency spectrum. Consequently, service providers are forced to find methods of enhancing the coverage and the capacity of their cellular networks. One basic approach is to build additional smaller cell sites to increase capacity. This is the primitive form of SDMA.

For a large geographical coverage a large number of mobile transceivers must be supported, the region is divided in a large number of cells[8]. This allows the same carrier frequency to be reused in different cells. A spatial distance to reduce the level of interference separates the signals at the same carrier frequency. Unfortunately, this can be a time consuming and expensive process, since building new cellular sites also includes finding and acquiring suitable base station site locations and extending the backbone infrastructure. Sectorization is another method of increasing capacity, but with associated tradeoffs in trunking efficiency and handoff rates. Sectorization has already been utilized to its practical limit in *many deployed cellular systems. In the existing cellular systems, 60° and 120° sectorized cells are used [7].*

A promising future method suggested is to utilize Adaptive Antennas, which has also been recognized as one potential economic approach. Adaptive base station antennas have been proposed as a means to achieve the requested longer range and higher capacity in cellular systems. These are important features to be considered when network operators open a new market or a new frequency band and are faced with the challenging task of building a complete cellular network from scratch. New operators must quickly create a cellular network that provides both coverage and capacity. To minimize the number of required sites, (i.e. minimizing the investments), these network operators must take advantage of every technique offering improvements of the communication quality. For established systems, Adaptive Antenna techniques can make use of existing cell sites, thus eliminating the costly step of deploying new sites for capacity enhancement.

1.2 Factors Limiting Performance of Wireless Communication Systems

Wireless communication systems are limited in performance and capacity by three major impairments: multipath fading, delay spread and co-channel interference [6]. Multipath fading is caused by the multiple paths that the transmitted signal can take to the received antenna. The signals from these paths add with different phases, resulting in a received signal amplitude and phase that vary with antenna location, direction, and polarization, as well as with time (with movement in the environment). This increases the required average received signal power for a given BER. Delay spread is the difference in propagation delays among the multiple paths. When the delay spread exceeds about 10 percent of the symbol duration, significant inter symbol interference can occur, which limits the maximum data rate.

Cellular systems divide the available frequency channels into channel sets, using one channel set per cell, with frequency reuse. This results in CCI, which increases as the number of channel sets decreases i.e. as the capacity of each cell increases. This is also known as MAI in case of CDMA. In CDMA, all the frequencies are present in a single cell, as the frequency reuse factor is one. Therefore, the CDMA systems are interference limited, that is, as the number of users increase, the interference gets increased.

1.3 Future Generation Multiple Access Techniques: CDMA & SDMA

For the past few years, adaptive beamforming for CDMA wireless communications has been drawing more and more attention from both the communications and antenna communities. There are a couple of reasons. First, CDMA standards for wireless communications systems are gaining acceptance from the industry, especially in North America[8]. Second, adaptive beamforming is highly suitable for a CDMA system, because the spreading codes can be used as references for beamforming.

CDMA is predicted to become an important method for the third generation wireless communication systems because of its potential capacity increase and anti-multipath fading capability [16]. However, for CDMA to satisfy the needs for an increased number of simultaneous users, a type of interference called MAI must be effectively combated. MAI is caused by the cross-correlation of user's spreading sequences. Although MAI could be eliminated by making the spreading sequences orthogonal among each other, multipath components and asynchronous transmission make them non-orthogonal again. So far, practical systems have used TPC to overcome fading and interference. The TPC maximizes the capacity of a cell by maintaining equal relative amplitudes among users at the base station receiver input. In the presence of fast fading, the power of the received signal falls considerably from its average level. During this condition, TPC alone will not suffice. To further improve the cell capacity by suppressing MAI from the received signal, interference reduction techniques such as interference cancellation using Adaptive Array Antennas, which is the ultimate form of SDMA is to be used in CDMA systems.

1.4 Objective

- To study the general beamforming concepts by analyzing the beampattern of matched filter beamformer for different element spacing and different array aperture
- To analyze the beampattern of non-adaptive beamformers like the tapered and optimum beamformer and study their performance in interference cancellation
- To analyze three different adaptive beamformers i.e. SMI, LMS, RLS algorithm.
- To derive and simulate the parameters of adaptive beamformers using Monte-Carlo simulation
- To design an adaptive antenna array with a new technique having features like
    - Low Sidelobes with Minimum Beamwidth
    - Steer able main beam without affecting the equal sidelobes
    - Fast Convergence
    - Flexibility

- Less Computational Complexity

- To prove the convergence by synthesizing Chebyshev beampattern for both even and odd number of elements
- To simulate the increase in CIR by reduction in interference power achieved using above technique

1.5 Literature Survey

Adaptive beamforming has been a subject of considerable interest for more than three decades. It has evolved into a mature technology. There are a number of textbooks and tutorial papers devoted to general concepts and applications of adaptive beamforming [2][3] [8][18]. In addition numerous papers and articles on specific techniques and applications can be found in open literature [13][10]. Thus, here some basic adaptive beamforming concepts and criteria are presented next.

The choice of the weight vector 'w' is based on the statistics of the signal vector x(t) received at the array as shown in figure 1.1. Basically, the objective is to optimize the beamformer response with respect to a prescribed criterion. So that the output y(t) contains minimal contribution from noise and interference. There are a number of criteria for choosing the optimum weights such as Minimum Mean Square Error (MMSE), Maximum Signal-to-interference Ratio (MSIR) and Minimum Variance (MV).

In MMSE method, the error between the beamformer output $w^H x(t)$ and the desired signal $d(t)$ is minimized. The characteristics of the desired signal correlates with it to a certain extent and this is called a reference signal. The weights are chosen to minimize the MSE between the beamformer output and the reference signal and the weights come out to be $w_{opt} = R^{-1} r$ where $R = E\{x(t)\, x^H(t)\}$ and $r = E\{d(t)\, x(t)\}$. Here w^{opt} is referred to as optimum wiener solution. In MSIR method, the weights can be chosen to directly maximize the signal-to-interference ratio (SIR). This criterion also leads to the same optimum wiener solution for the weights.

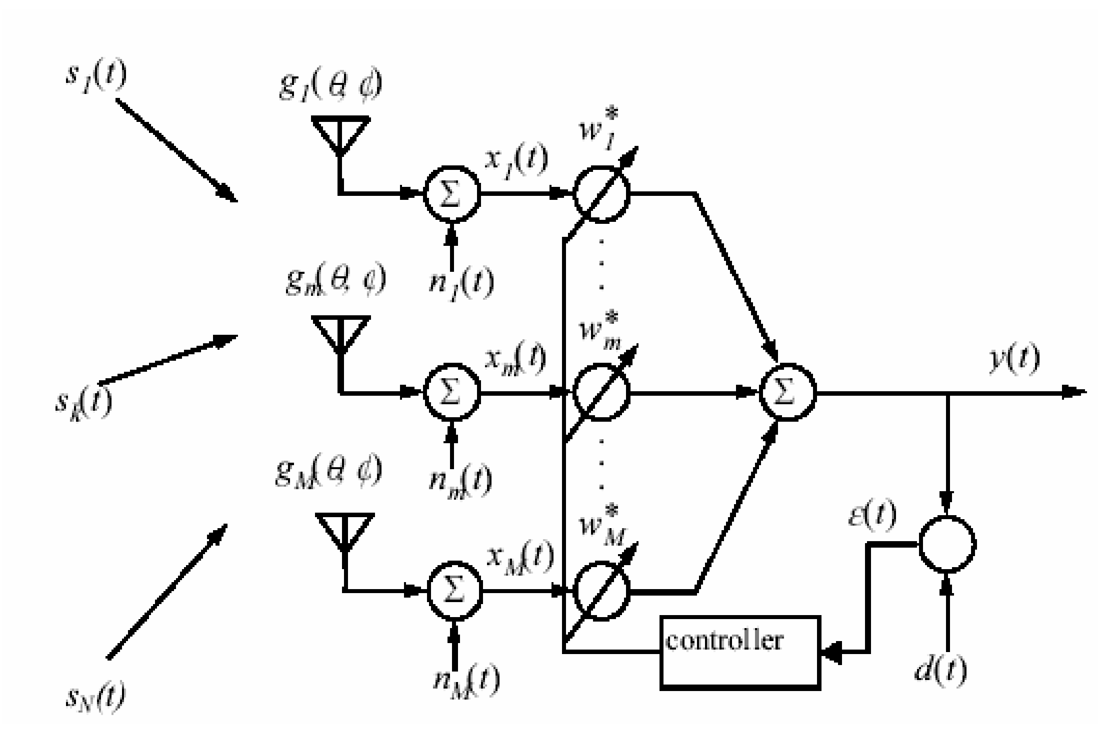

Figure 1.1: Block Diagram of adaptive beamforming system

If the desired signal and its direction are both unknown, the way to ensure a good signal reception is to minimize the output noise variance. To ensure that the desired signal is passed with a specific gain and phase, a constraint may be used so that the response of the beamformer is $w^H v = g$. If $g=1$ the response of the beamformer is often termed as minimum variance distortion less response (MVDR) beamformer. The solution for the optimal weights in all three cases is the same. The fact that the optimum weights using different criteria are all given by the Wiener solution demonstrates the fundamental importance of the Wiener-Hopf equation in establishing the theoretical adaptive beamforming steady-state performance limits.

All these beamforming techniques are used to null the interferers as many as possible, which is limited due to the limited number of antenna elements in the antenna array. For the WCDMA system, where the number of interferers is very large, a different criterion is required with which the sidelobe levels can be reduced instead of creating nulls. Therefore, flexible sidelobe topography is the need of these systems for interference cancellation. The algorithm analyzed in this thesis an algorithm based on uniform linear array (ULA) is analyzed for creating low sidelobes. This algorithm is able to taper the sidelobes to any desired level having minimum possible main lobe beamwidth with a fast convergence speed. It has the flexibility to reduce the interference power from any specific direction to a very low level if large number of interferers is present in a specific direction.

1.6 Thesis Organization

In chapter 2, the general concepts of conventional beamforming, that is, the spatial discrimination or filtering of signals collected with a sensor array, is introduced. In conventional or non-adaptive beamforming the effect of parameters such as element spacing, resolution, and sidelobe level that affect its performance is also discussed.

In chapter 3 non-adaptive alternatives that can be employed in certain cases, namely, the use of a taper with the spatial matched filter is discussed. Other non-adaptive method that is the optimum beamformer, which is based on a priori knowledge of the data statistics, is also discussed. The use of taper in optimum beamforming is explained with optimum beamformer.

In chapter 4, the use of adaptive methods of beamforming, that are based on collected data from which the correlation matrix is estimated, is discussed. Three adaptive algorithms SMI, LMS, RLS are described and their performance parameters are discussed along with the parameter simulation of SMI algorithm.

In chapter 5, a novel two-step tapered beamforming algorithm is analyzed for flexible sidelobe adjustment. This algorithm is used to synthesize the Chebyshev pattern for equal sidelobe levels with a very fast convergence rate. This is finally used to increase the capacity of a CDMA system by reducing the interference level of large number of interferers present in the system by presenting low sidelobe to all the undesired users.

Chapter 6 enlists the conclusion and the future scope of the present work.

Chapter 2

Conventional Beamforming Techniques

In this chapter, the general concepts of conventional beamforming, that is, the spatial discrimination or filtering of signals collected with a sensor array, is introduced. In conventional or non-adaptive beamforming the effect of parameters such as element spacing, resolution, and sidelobe level that affect its performance is also discussed.

2.1 Introduction

The term beamforming relates to the function performed by a device or apparatus in which energy radiated by an aperture antenna is focused along a specific direction in space [8]. The objective is either to preferentially receive a signal from that direction or to preferentially transmit a signal in that direction. In many applications of antennas, point-to-point communications is of interest. A highly directive antenna beam can be used to advantage. The direction beam can be realized by forming an array with a number of elemental radiators. As the directivity of the antenna increases, the gain also increases. At the receive end of the communication link, the increase in directivity means that the antenna receives less interference from its signal environment. It is clear that high gain antennas have significant advantage in point-to-point communication circuits.

2.2 Array Signal Model

Consider a signal received by the uniform linear array (i.e. the array of equally spaced antenna elements) from an angle Φ as shown in figure 2.1. Each sensor receives the spatially propagating signal and converts its energy into voltage. The discrete time signals from a ULA can be written as:

$$X(n) = [x_1(n)x_2(n)..........x_M(n)] \tag{2.1}$$

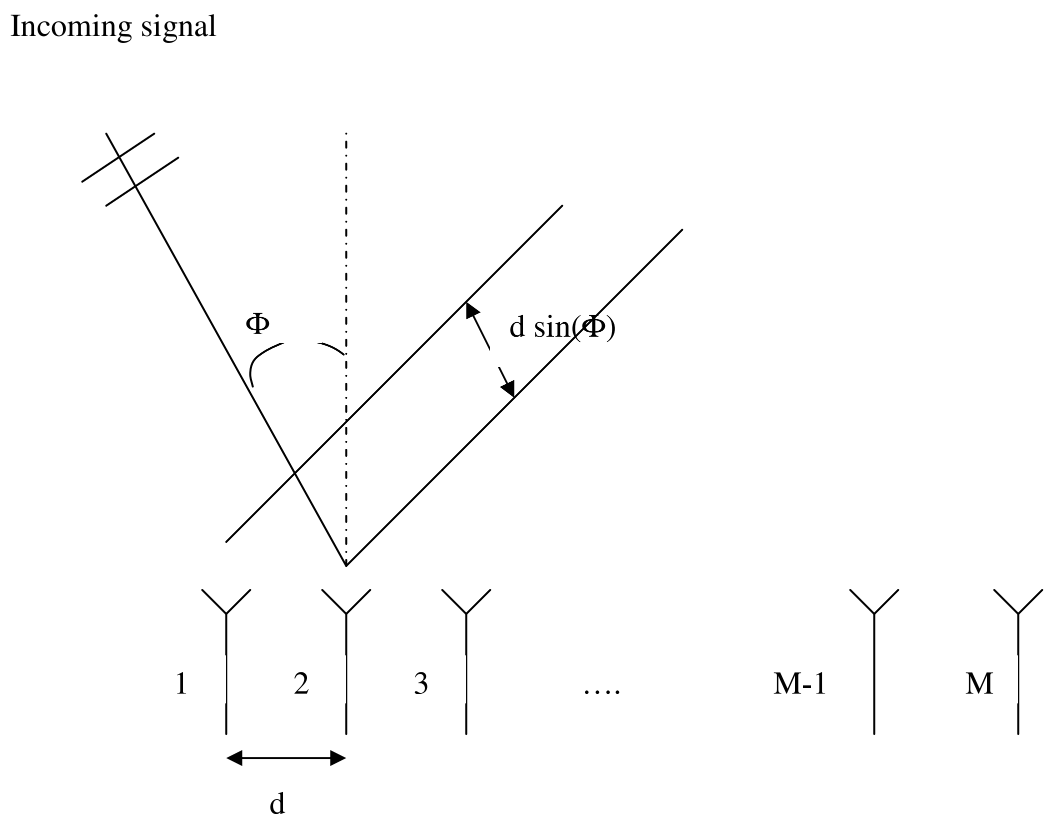

Figure 2.1. Plane wave impinging on a uniform linear array

Where M is the total number of sensors. A single measurement of this signal is called an array snapshot. Let us begin by examining a single, carrier-modulated signal arriving from angle Φ_s that is received by the m_{th} sensor [3].

$$s_m(t) = s_o(t)\cos(2\pi f_c t) \tag{2.2}$$

It is assumed that the signal $s_o(t)$ has deterministic amplitude and random uniformly distributed phase. The received signal is given as

$$x_m(t) = h_m(t, \Phi_s) * s_m(t - \tau_m) + w_m(t) \tag{2.3}$$

where $h_m(t,\Phi_s)$ is the impulse response of the m_{th} sensor as a function of both time and angle Φ_s and w_m is the sensor noise. Here the relative delay τ_m at the m_{th} sensor is also a function of Φ_s. Usually τ_1=0, in which case the delays to the remaining sensors (m=2,3….., M) are simply the differences in propagation time of $s_o(t)$ to these sensors with respect to the first sensor. The sensor signal in frequency domain can be expressed as

$$X_m(F) = H_m(F_c,\Phi_s)S_o(F)e^{-2\pi f_c \tau_m} + W_m(F) \tag{2.4}$$

and the discrete time signal model is obtained by sampling the inverse Fourier transform of (2.4), which can be written as

$$x_m(n) = H_m(F_c)s_o(n)e^{-2\pi f_c \tau_m} + w_m(n) \tag{2.5}$$

If it is further assumed that each sensor in the array has an equal, omni directional response at frequency F_c, then the constant sensor responses can be absorbed in a single term

$$s(n) = H(F_c)s_o(n) \tag{2.6}$$

The full array discrete time signal model as

$$x(n) = \sqrt{M}\,v(\Phi_s)s(n) + w(n) \tag{2.7}$$

Where

$$v(\Phi_s) = 1/\sqrt{M}\,[1\; e^{-2\pi f_c \tau_1} \ldots\ldots\ldots\ldots e^{-2\pi f_c \tau_M}\;] \tag{2.8}$$

is the array response vector. Here the normalization is used for mathematical convenience so that the array response vector has unit norm, that is $[v\,(\phi_s)]^2 = 1$.

The interelement spacing between equally spaced elements is denoted by ‘d’. The time delay between spatial signal arriving at an angle Φ_s is $\tau(\Phi_s) = d\sin(\Phi_s)/c$ where c is the rate of propagation of the signal. As a result the delay to the m_{th} sensor is given by

$$\tau_m = \frac{(m-1)d\sin(\Phi)}{c} \tag{2.9}$$

And substituting into (2.8), the array response for a ULA is

$$v(\Phi) = \frac{1}{\sqrt{m}}[1 \quad e^{-j2\pi[(d\sin(\Phi)/\lambda]} \ldots\ldots\ldots\ldots\ldots e^{-j2\pi[(d\sin(\Phi)/\lambda](m-1)}]^T \tag{2.10}$$

Since $f_c = c/\lambda$.

2.3 Conventional Beamforming

In communication the desired information to be extracted from an array of sensors is the message contained in the signal. To this end, it is required to linearly combine the signals arriving from a specific angle. This operation shown in figure 2.2 is known as beamforming because the weighting process emphasizes signals from a particular direction while attenuating those from other directions and can be thought of as casting or forming a beam. In this sense, a beamformer is a spatial filter; and in the case of a ULA, it has a direct analogy to an FIR frequency selective filter for temporal signals. Beamforming is commonly referred to as "electronic" steering since the weights are applied using electronic circuitry following the reception of signal for the purpose of steering the array in a particular direction.

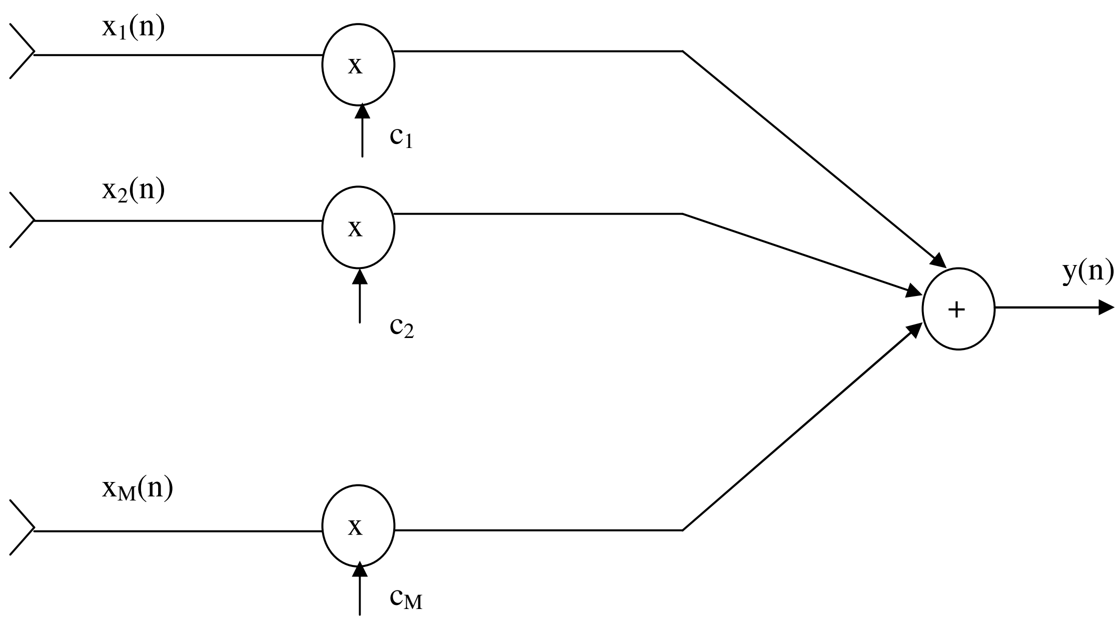

Figure 2.2 Beamforming operation

The response of the beamformer is analyzed by a weight vector c as a function of angle Φ_s and it is given by

$$Y(n) = c^H x(n) = Mc^H v(\Phi_s) s(n) + w(n) \tag{2.11}$$

where $$c = [c_1 c_2 c_3 .... c_M]^T \tag{2.12}$$

is the column vector of beamforming weights.

The beamformer output power is given by

$$P_y = E[y(n)^2] = c^H R_x c \tag{2.13}$$

$$\text{where} \quad R_x = E[x(n)x^H(n)] \tag{2.14}$$

is the correlation matrix of the array signal x(n). SNR in each element is given by

$$\mathrm{SNR}_{\mathrm{element}} = \frac{\sigma_s^2}{\sigma_w^2} = \frac{[e^{-j2\Pi(m-1)u_s} s(n)]^2}{E\{w(n)^2\}} \tag{2.15}$$

Where σ_s^2 =E{s (n)^2} and σ_w^2=E {w(n)^2} are the element level signal and noise powers. Now if the signals at the output of the beamformer are considered, the signal and noise powers are given by

$$P_s = E\{\sqrt{M}[c^H v(\Phi)]s(n)\}^2 = M\sigma_s^2[c^H v(\Phi)]^2 \tag{2.16}$$

$$P_n = E\{c^H w(n)\}^2 = c^H R_n c = [c]^2 \sigma_w^2 \tag{2.17}$$

Because $R_n = \sigma_w^2 I$. Therefore, the resulting SNR at the output, known as array SNR, is

$$\mathrm{SNR}_{\mathrm{array}} = P_s / P_n = \frac{M.\mathrm{SNR}_{\mathrm{element}}}{[c]^2}[c^H v(\Phi)]^2 \tag{2.18}$$

Which is simply the product of the beamforming gain and the element level SNR.Thus, the beamforming gain is given by

$$G_{bf} = \frac{\mathrm{SNR}_{\mathrm{array}}}{\mathrm{SNR}_{\mathrm{element}}} = \frac{[c^H v(\Phi)]^2}{[c]^2} M \tag{2.19}$$

The beamforming gain is strictly a function of angle of arrival φ_s of the desired signal, the beamforming weight vector c, and the number of sensors M.

2.4 Spatial Matched Filtering or Steering Vector Beamformer

The array signal model of a single signal, arriving from a direction Φ_s, with sensor thermal noise is given as

$$x(n) = \sqrt{M} v(\Phi_s) s(n) + w(n) \tag{2.20}$$

Where the components of the noise vector w (n) are uncorrelated and have power σ_w^2. The individual elements of the array contain the same signal s (n) with different phase shifts corresponding to the differences in propagation times between elements. Ideally the signals from the M array sensors are added coherently, which requires that each of the relative phases be zero at the point of summation; that is, s (n) is added with a perfect replica of itself. Thus a set of complex weights is needed that result in a perfect alignment of all sensor signals. The beamforming weight vector that phase aligns a signal from direction Φ_s at the different array elements is the steering vector, which is simply the array response vector in that direction, that is,

$$c_{mf}(\Phi_s) = v(\Phi_s) \qquad (2.21)$$

This steering vector beamformer is also known as the spatial matched filter since the steering vector is matched to the array response of signals impinging on the array from an angle Φ_s. As a result, Φ_s is known as the look direction. The use of the spatial matched filter is commonly referred to as conventional beamforming.The output of spatial matched filter is

$$y(n) = c_{mf}^H(\Phi_s)x(n) = v^H(\Phi_s)x(n) \qquad (2.22)$$

By substituting x (n) and v (Φ_s) from equations (2.7) and (2.8) respectively,

$$y(n) = \sqrt{M}\, s(n) + \tilde{w}(n) \qquad (2.23)$$

where $\tilde{w}(n) = c_{mf}^H(\Phi_s)w(n)$ is the beamformer output noise. The array SNR of the spatial matched filter output can be written as

$$\begin{aligned} SNR_{array} &= \frac{P_s}{P_n} = \frac{M\sigma_s^2}{E[v^H(\Phi_s)w(n)]^2} = \frac{M\sigma_s^2}{v^H(\Phi_s)R_n v(\Phi_s)} \\ &= M\frac{\sigma_s^2}{\sigma_w^2} = M.SNR_{elem} \end{aligned} \qquad (2.24)$$

The beamforming gain is G_{bf} = M, that is, equal to the number of sensors. In the case of spatially white noise, the spatial matched filter is optimum in the sense of maximizing the SNR at the output of the beamformer. Thus, the beamforming gain of the spatial matched filter is known as array gain because this is the maximum possible gain of a signal with respect to sensor thermal noise for a given array. The gain is limited due to limitation on the number of array elements.

The spatial matched filter or the conventional beamformer maximizes the SNR because the individual sensor signals are coherently aligned prior to their combination. The other sources of interference that have spatial correlation require other type of adaptive beam formers that maximizes the signal to interference plus noise ratio (SINR).

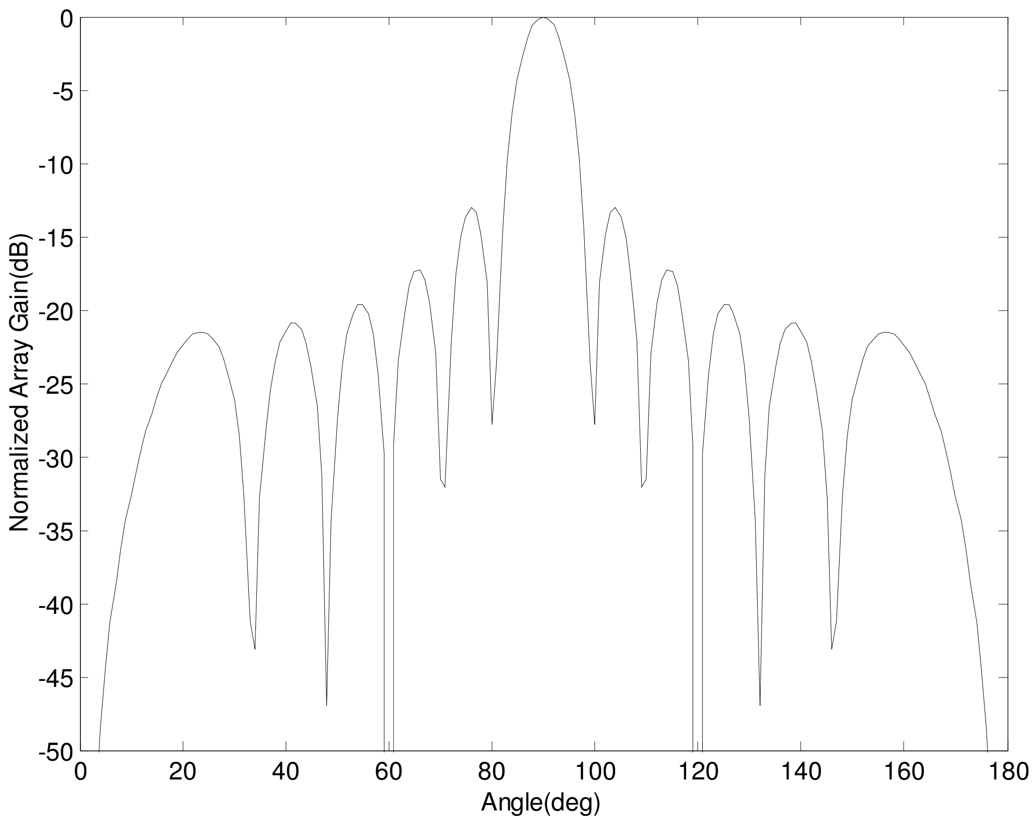

Figure 2.3 A sample beam pattern of a spatial matched filter for an M=12 element ULA steered to $\Phi = 90^o$

2.5 Beam Response

A standard tool for analyzing the performance of a beamformer is the response for a given weight vector 'c' as a function of angle Φ, known as the beam response. This angular response is computed by applying the beamformer c to a set of array response vectors from all possible angles, that is, $0 \le \Phi \le 180^o$,

$$C(\Phi)=c^H v(\Phi) \tag{2.25}$$

Typically, in evaluating a beamformer, the quantity $|C(\Phi)|^2$ is required, which is known as the beam pattern. A sample beam pattern for a 12-element uniform array with uniform weighting ($c_m=1/\sqrt{M}$) is shown in fig. 2.3, which is plotted on a logarithmic scale in decibels. The large main lobe is centered at $\Phi = 90^o$, the direction in which the array is steered.

2.6 Analysis of Beampattern

The beam pattern of the spatial matched filter can illustrate several key performance metrics of an array [12]. The first and most obvious attribute is the large lobe centered on Φ_s, known as the main lobe or main beam, and the remaining, smaller peaks are known as side lobes. The value of beam pattern at the desired angle $\Phi = \Phi_s$ is equal to 1(0 dB) due to the normalization used in the computation pf the beam pattern. A response of less than 1 in the look direction corresponds to a direct loss in desired signal power at the beamformer output. The sidelobe levels determine the rejection of the beamformer to signals not arriving from the look direction. The second attribute is the beam width, which is the angular span of the main beam. The resolution of the beamformer is determined by this main lobe width, with smaller beam widths resulting in better angular resolution

2.7 Effect of element spacing

The element spacing must be $d \le \lambda/2$ to prevent spatial aliasing. The beam patterns of spatial matched filter for ULAs with element spacing of $\lambda/4$, $\lambda/2$, λ, and 2λ(equal-sized apertures of 10λ with 40, 20, 10, and 5 elements, respectively) are shown in figure 2.4.it can be noted that the beam pattern for $\lambda/4$ and $\lambda/2$ spacing are identical with equal-sized main lobes and the first sidelobe having a height of –13dB. The over sampling for the array with an element spacing of $\lambda/4$ provides no additional information and therefore does not improve the beamformer response in terms of resolution. In case of the under sampled arrays ($d=\lambda$ and 2λ), it can be seen that the same structure (beam width) around the look direction but also note the additional peaks in the beam pattern (0 dB) at 0°and 180° for d=λ and in even closer for d=2λ. These additional lobes in the beam pattern are known as grating lobes. Grating lobes create spatial ambiguities; that is, signals incident on the array from the angle associated with a grating lobe will look just like signals from the direction of interest. The beamformer has no means of distinguishing signals from these various directions. In certain applications, grating lobes may be acceptable if it is determined that it is either impossible or very improbable to receive returns from these angles; for example, a communications satellite is unlikely to receive signals at angles other than those corresponding to the ground below. The benefit of the larger element spacing is that the resulting array has a larger aperture and thus better resolution. The topic of larger apertures with element spacing greater than λ/2 is commonly referred to as a thinned array [3].

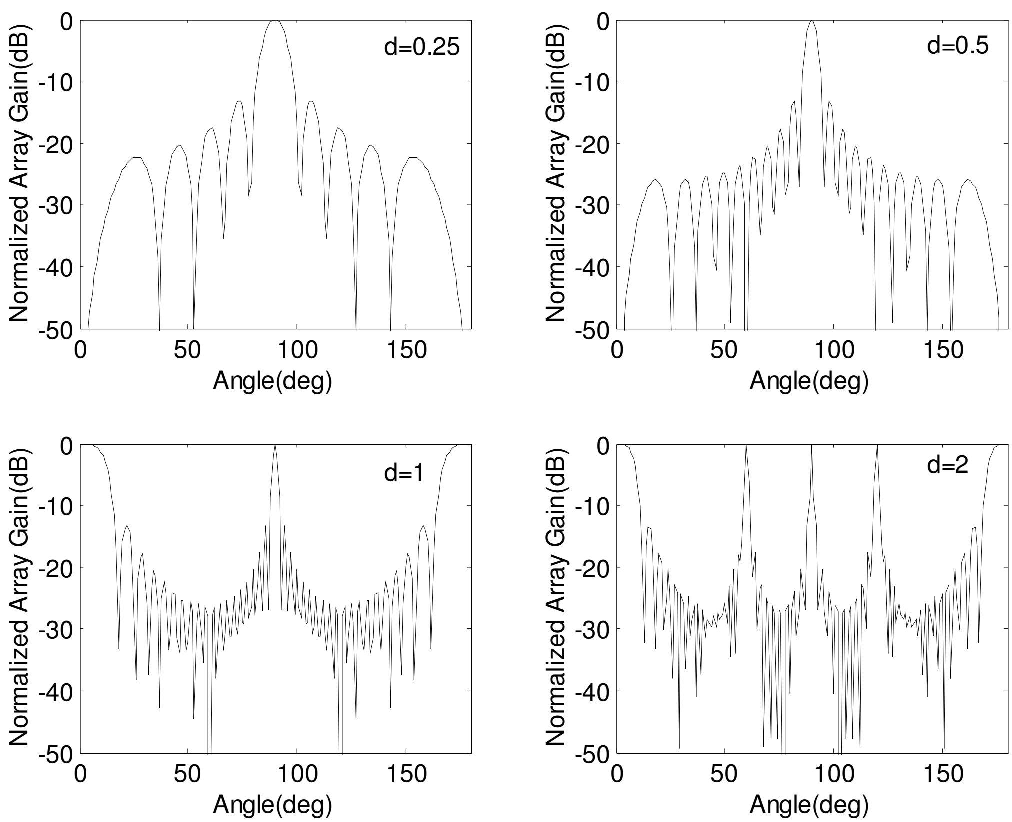

Figure 2.4 Beam patterns of a spatial matched filter for different element spacing with an equal-sized aperture L =10λ

2.8 Array Aperture and Beamforming Resolution

The aperture is the finite area with a sensor collects spatial energy [1]. In the case of a ULA, the aperture is the distance between the first and last elements. In general, the designer of an array yearns for as much aperture as possible. The greater the aperture, the finer the resolution of the array, which is its ability to distinguish between closely spaced sources. Improved resolution results in better angle estimation capabilities. The angular resolution of a sensor array is measured in beam width Δ_{ϕ}, which is commonly defined as the angular extent between the nulls of the main beam $\Delta_{\phi nm}$, or the half power points of the main beam (-3dB) $\Delta_{\phi 3dB}$. As a general rule of thumb, the –3dB beam width for an array with an aperture length of L is quoted in radians as

$$\Delta\Phi_{3dB} \approx \lambda / L \tag{2.26}$$

Although the actual –3dB points of a spatial matched filter yields a resolution of $\Delta_{\phi 3dB} = 0.89\lambda/L$ (the resolution of the conventional matched filter near broadside, ϕ=90°). The approximation in (2.26) is intended for the full range of prospective beam formers, not just spatial matched filters. Since the resolution is dependent on the operating frequency F_c or equivalently on the wavelength, the aperture is often measured in wavelengths rather than in absolute length in meters. At large operating frequencies, say F_c = 10GHz or λ = 3cm (X band in radar terminology), it is possible to populate a physical aperture of fixed length with a large number of elements, as opposed to lower operating frequencies say, Fc = 300MHz or λ = 1m.

The effect of aperture on radiation is shown using a few representative beam patterns. Figure 2.5 shows beam patterns for M = 4, 8, 16 and 32 with interelement spacing fixed at $d=\lambda/2$ (nonaliasing condition). Therefore, the corresponding apertures in wavelengths are D=2λ, 4λ, 8λ and 16λ. Clearly, increasing the aperture yields better resolution with a factor of 2 improvements for each of the successive twofold increases in aperture length. The level of the first sidelobe is always about –13dB below the main lobe peak.

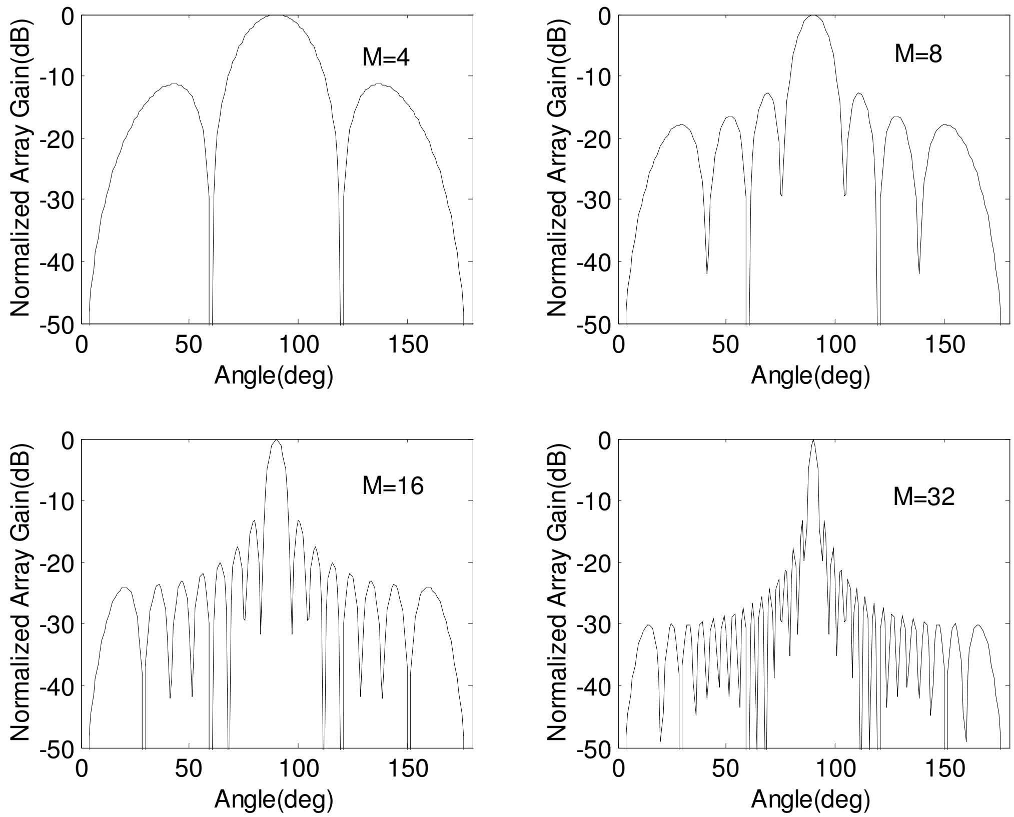

Figure 2.5 Beam patterns of a spatial matched filter for different aperture sizes with a common element spacing of d = λ/2

Chapter 3

Interference Cancellation using Non-Adaptive Beamforming Techniques

The interference level can be reduced by means of various adaptive and non-adaptive beamforming methods. In this chapter non-adaptive alternative that can be employed in certain cases, namely, the use of a taper with the spatial matched filter is discussed. Other non-adaptive method that is the optimum beamformer, which is based on a priori knowledge of the data statistics, is also discussed.

3.1 Tapered Beamforming

The spatial matched filter would be perfectly sufficient if the only signal present, aside from the sensor thermal noise, were the signal of interest [3]. However, in many instances, it must be contended with other, undesired signals that hinder our ability to extract the signal of interest. These signals may also be spatially propagating at the same frequency as the operating frequency of the array. Such signals are referred as interference. These signals may be present due to hostile adversaries that are attempting to prevent us from receiving the signal of interest, for example. Jammers in radar or communications or they might be incidental signals that are present in our current operating environment, such as transmissions by other users in a communications system or radar clutter.

However, there are also non-adaptive alternatives that can he employed in certain cases, namely, the use of a taper with the spatial matched filter.

3.1.1 Example of Tapered Beamformer

Consider the ULA signal model from (2.20), but now including an interference signal i(n) made up of P interference sources

$$x(n) = s(n) + i(n) + w(n) = \sqrt{M}v(\phi_s)s(n) + \sqrt{M}\sum_{P=1}^{P} v(\phi_P H_P(n)) + w(n) \tag{3.1}$$

where v (Φ_p) and $i_p(n)$ are the array response vector and actual signal due to the pth interferer respectively. If a ULA is assumed with $\lambda/2$ element spacing, the beampattern of the spatial matched filter, as shown in Figure 3.1, may have sidelobes that are high enough to pass these interferers through the beamformer with a high enough gain to prevent us from observing the desired signal. For this array, if an interfering source were present at $\phi=20^o$ with a power of 40 dB, the power of the interference at the output of the spatial matched filter would be 20 dB because the sidelobe level at $\phi=20°$ is only -20 dB. Therefore, if a weaker signal is being received from ϕ_s = 90°, it will be unable to extract it because of sidelobe leakage from this interferer.

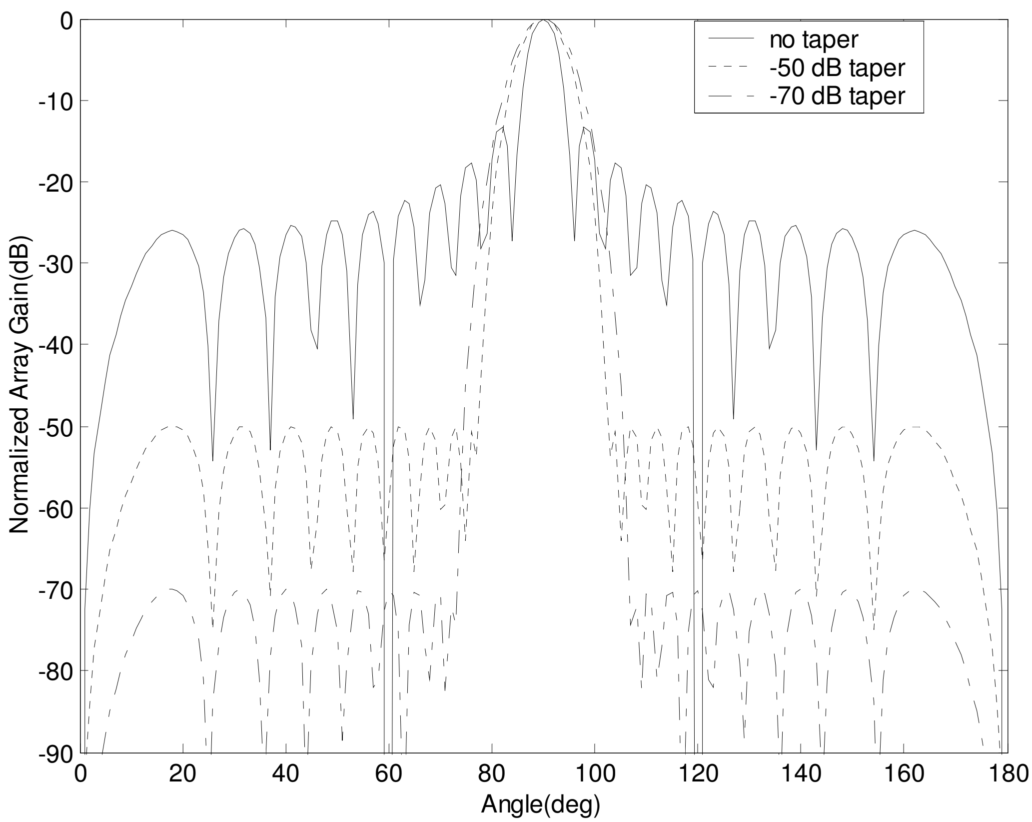

Figure 3.1: Beam patterns of beam formers with M=20 with no taper (solid line), -50 dB taper (dashed line), and –70dB taper (dash-dot line)

The spatial matched filter has weights all with a magnitude equal to $1/\sqrt{M}$. The look direction is determined by a linear phase shift across the weights of the spatial matched filter. However, the sidelobe levels can be further reduced by tapering the magnitudes of the spatial matched filter. To this end, a tapering vector **t** is applied to the spatial matched filter to realize a low sidelobe level beamformer

$$c_{tbf}(\phi_s) = t\Theta c_{mf}(\phi_s) \tag{3.2}$$

Where Θ represents the Hadamard product, which is the element-by-element multiplication of the two vectors. This beamformer is referred as the tapered beamformer.

The determination of a taper can be thought of as the design of the desired beamformer where c_{mf} simply determines the desired angle. The weight vector of the spatial matched filter from equation (2.21) has unit norm; that is, $c_{mf}^H c_{mf} = 1$. Similarly, the tapered beamformer c_{tbf} is normalized so that

$$c_{tbf}^H(\phi_s)c_{tbf}(\phi_s) = 1 \tag{3.3}$$

Here, Dolph Chebyshev tapers are used for illustration purpose. This taper produces a constant side lobe level (equiripples in the stop band in spectral estimation), which is often a desirable attribute of a beamformer. The best taper choice is driven by the actual application. The beam patterns of the ULA are used again, but this time the beam patterns of tapered beam formers are also shown in Figure 3.1. The sidelobe levels of the tapers were chosen to be -50 and -70 dB. The same 40dB interferer would have been reduced to -10 and -30 dB at the beamformer output, respectively.

However, the use of tapers does not come without a cost. The peak of the beam pattern is no longer at 0 dB. This loss in gain in the current look direction is commonly referred to as a tapering loss and is simply the beam pattern evaluated at ϕ_s.

$$L_{taper} \stackrel{\Delta}{=} \left|C_{tbf}(\phi_s)\right|^2 = \left|c_{tbf}^H(\phi_s)v(\phi_s)\right|^2 \tag{3.4}$$

Since the tapering vector was normalized as in (3.3), the tapering loss is in the range $0 \le L_{taper} \le 1$ with $L_{taper} = 1$ corresponding to no loss (untapered spatial matched tilter). The tapering loss is the loss in 'SNR' of the desired signal at the beamformer output that cannot be recovered. More significantly, notice that the main lobes of the beam patterns in Figure 3.1 are much broader for the tapered beam formers. The consequence is a loss in resolution that becomes more pronounced as the tapering is increased to achieve lower sidelobe levels. Its interpretation for an array can better be understood by examining plots of the magnitude of the taper vector **t**, shown in Figure 3.2 for the -50- and -70- dB Dolph-Chebyshev tapers. Note that the elements on the ends of the array are given less weighting as the tapering level is increased. The tapered array in effect de-emphasizes these end elements while emphasizing the center elements. Therefore, the loss in resolution for a tapered beamformer might be interpreted as a loss in the effective aperture of the array imparted by the tapering vector.

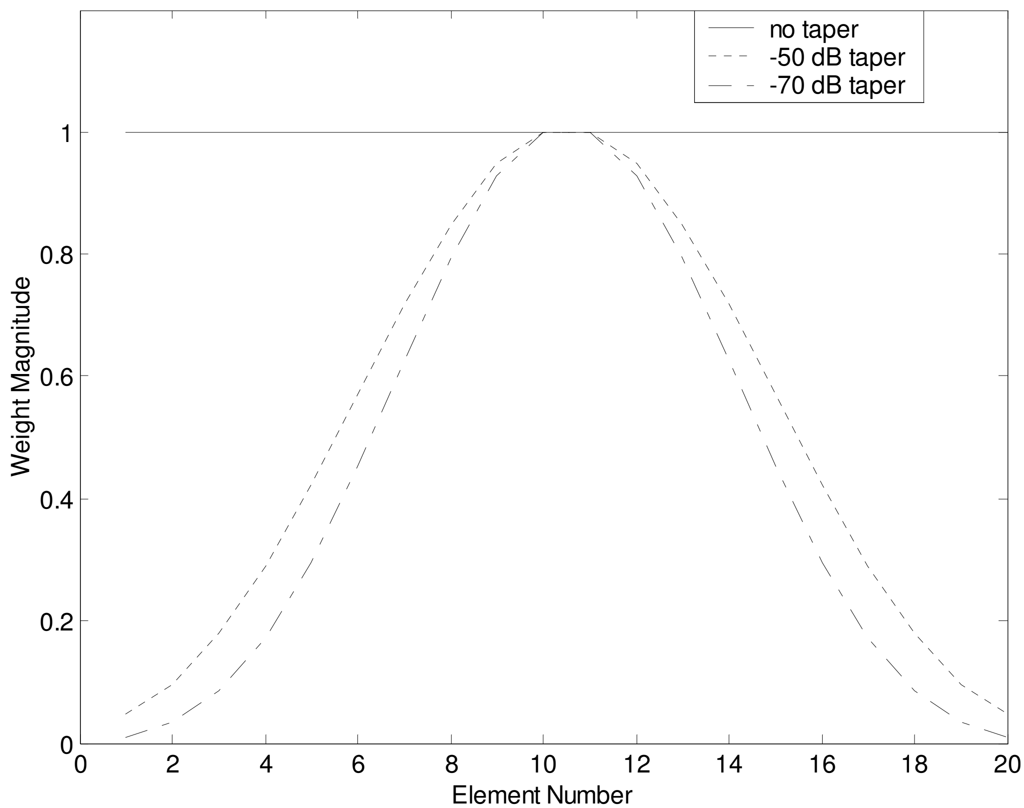

Figure 3.2: The magnitude levels of the tapered beamforming weights as a function of element number for M=20 with no taper (solid line), -50-dB taper (dashed line), and -70-dB taper (dash-dot line)

3.2 Optimum Array Processing

So far, beamformers whose weights are determined independently of the data to be processed are considered. If instead the actual beamforming weights are based on the array data themselves, then the result is an adaptive array and the operation is known as adaptive beamforming. Ideally, the beamforming weights are adapted in such a way as to optimize the spatial response of the resulting beamformer based on a certain criterion. To this end, the criterion is chosen to enhance the desired signal while rejecting other, unwanted signals. This weight vector is similar to the optimum matched filter [10].

Optimum array processing methods make use of the a priori known statistics of the data to derive the beamforming weights. Implicit in the optimization is the a priori knowledge of the true statistics of the array data. The general term adaptive is used to refer to beamformers that use an estimated correlation matrix computed from array snapshots while reserving the term optimum for beamformers that optimize a certain criterion based on knowledge of the array data statistics. The array signal model that contains interference in addition to the desired signal and noise is discussed first. Then the optimum beamformer is derived where the optimality criterion is the maximization of the theoretical signal-to-interference-plus-noise ratio.

The signal of interest is seldom the only array signal aside from thermal noise present. The array must often contend with other, undesired signals that interfere with our ability to extract this signal of interest. Often the interference is so powerful that even a tapered beamformer is unable to sufficiently suppress it to extract the signals of interest. The determination of the presence of signals of interest is known as detection, while the inference of their parameters; for example, the angle of arrival ϕ_s is referred to as estimation. The topic of detection is not explicitly treated here. Rather, the visibility of the desired signal is maximized at the array output, that is, the ratio of the signal power to that of the interference plus noise, to facilitate the detection process.

Consider an array signal that consists of the desired signal s (n), an interference signal i(n),along with sensor thermal noise w(n), that is,

$$x(n) = s(n) + i(n) + w(n) = \sqrt{M}\,v(\phi_s)s(n) + i(n) + w(n) \qquad (3.5)$$

Where s (n) is a signal with deterministic amplitude σ_s and uniformly distributed randomphase. The interference-plus-noise component of the array signal is

$$x_{i+n}(n) = i(n) + w(n) \tag{3.6}$$

Which are both modeled as zero-mean stochastic processes. The interference has spatial correlation according to the angles of the contributing interferers while the thermal noise is spatially uncorrelated. The sensor thermal noise is assumed to be uncorrelated with power σ_w^2. The assumption is made that all of these three components are mutually uncorrelated. As a result, the array correlation matrix is

$$R_x = E\{x(n)x^H(n)\} = M\sigma_s^2 v(\phi_s)v^H(\Phi_s) + R_i + R_n \tag{3.7}$$

Where σ_s^2 is the power of the signal of interest and R_i and R_n are the interference and noise correlation matrices, respectively. The interference-plus-noise correlation matrix is the sum of these latter two matrices

$$R_{i+n} = R_i + R_n \tag{3.8}$$

Where $R_n = \sigma_w^2 I$ since the sensor thermal noise is spatially uncorrelated.

3.2.1 Optimum Beamforming

The ultimate goal of the prospective adaptive beamformer is to combine the sensor signals in such a way that the interference signal is reduced to the level of the thermal noise while the desired signal is preserved. Stated another way, it is required to maximize the ratio of the signal power to that of the interference plus noise, known as the SINR, maximizing the SINR is the optimal criterion for most detection and estimation problems. Simply stated, maximizing the SINR seeks to improve the visibility of the desired signal as much as possible in a background of interference. This criterion should not be confused with maximizing the SNR *(spatial matched filter) in the absence of interference [3]. At the input of the array, that is, in each individual sensor, the SINR is given by*

$$\mathrm{SINR}_{\mathrm{elem}} = \frac{\sigma_s^2}{\sigma_i^2 + \sigma_w^2} \tag{3.9}$$

Where σ_s^2, σ_i^2, and σ_w^2 are the signal, interference, and thermal noise powers in each individual element. The SINR at the beamformer output, following the application of the beamforming weight vector c is

$$SINR_{out} = \frac{(c^H s(n)^2}{E\left\{\left|c^H x_{i+n}(n)\right|^2\right\}} = \frac{M\sigma_s^2\left|c^H v(\phi_s)\right|^2}{c^H R_{i+n} c} \tag{3.10}$$

This array output SINR is maximized. First, note that the interference-plus-noise correlation matrix can be factored as

$$R_{i+n} = L_{i+n} L_{i+n}^H \tag{3.11}$$

where L_{i+n} is the Cholesky factor of the correlation matrix. Thus, defining

$$\tilde{c} = L_{i+n}^H c \tag{3.12}$$

$$\tilde{v}(\phi_s) = L_{i+n}^{-1} v(\phi_s) \tag{3.13}$$

(3.10) can be written as

$$\mathrm{SINR}_{\mathrm{out}} = \frac{\mathrm{M}\sigma_s^2\left|\tilde{\mathrm{c}}^{\mathrm{H}}\,\tilde{\mathrm{v}}(\phi_s)\right|^2}{\tilde{\mathrm{c}}^{\mathrm{H}}\,\tilde{\mathrm{c}}} \tag{3.14}$$

Using the Schwartz inequality

$$\tilde{c}^H\,\tilde{v}(\phi_s) \le \left\|\tilde{c}\right\|\,\left\|\tilde{v}(\phi_s)\right\| \tag{3.15}$$

And substituting (3.15) into (3.14),

$$\mathrm{SINR}_{\mathrm{out}} \le \mathrm{M}\sigma_s^2\,\frac{\left\|\tilde{\mathrm{c}}\right\|^2\left\|\tilde{\mathrm{v}}(\phi_s)\right\|^2}{\left\|\tilde{\mathrm{c}}\right\|^2} = \mathrm{M}\sigma_s^2\left\|\tilde{\mathrm{v}}(\phi_s)\right\|^2 \tag{3.16}$$

Thus, the maximum SINR is found by satisfying the upper bound for (3.16), which yields

$$\mathrm{SINR}_{out}^{max} = M\sigma_s^2 \tilde{v}^H(\phi_s)\,\tilde{v}(\phi_s) = M\sigma_s^2\left[v^H(\phi_s)R_{i+n}^{-i}v(\phi_s)\right] \tag{3.17}$$

The same maximum SINR is obtained if $\tilde{c} = \alpha\,\tilde{v}(\phi_s)$ where α is an arbitrary constant. In other words, the SINR is maximized when these two vectors are parallel to each other and α can be chosen to satisfy other requirements. Therefore using (3.13), the optimum weight vector.

$$c_o = \alpha L_{i+n}^{-H}\tilde{v}(\Phi_s) = \alpha R_{i+n}^{-1}v(\Phi_s) \tag{3.18}$$

Where α is an arbitrary constant. Thus, the optimum beamforming weights are proportional to $R_{i+n}^{-1}v(\phi_s)$. The proportionality constant α in (3.18) can be set in a variety of ways.Table 3.1 gives various normalizations for the optimum beamformer. The normalization adopted throughout this chapter is to constrain the optimum beamformer to have unity gain in the look direction, that is, $c_0^H v(\phi_s) = 1$. Therefore,

$$c_0^H v(\phi_s) = \alpha\left[R_{i+n}^{-1}v(\phi_s)^H\right]v(\phi_s) = 1 \tag{3.19}$$

And the resulting optimum beamformer is given by

$$c_0 = \frac{R_{i+n}^{-1}v(\phi_s)}{v^H(\phi_s)R_{i+n}^{-1}v(\phi_s)} \tag{3.20}$$

In general, the normalization of the optimum beam former is arbitrary and is dictated by the use of the output, for example, measure residual interference power or detection. In any case, the SINR is maximized independently of the normalization. The most commonly used normalizations are listed in Table 3.1.

Alternately, the optimum beamformer can be derived by solving the following constrained optimization problem: Minimize the interference-plus-noise power at the beamformer output

$$P_{i+n} = E\left\{\left|c^H x_{i+n}(n)\right|^2\right\} = c^H R_{i+n} c \tag{3.21}$$

subject to a look-direction distortion less response constraint, that is,

$$\min P_{i+n} \qquad \text{subject to} \qquad c^H\, v(\phi_s) = 1 \tag{3.22}$$

The solution of this constrained optimization problem is found by using Lagrange multipliers and results in the same weight vector. This formulation has led to the commonly used term MVDR beamforming.

TABLE 3.1

Optimum weight normalizations for unit gain in look direction, Unit gain on noise, and unit gain on interference-plus-noise constraints.

Constraint	**Mathematical Formulations**	**Optimum Beamformer Normalization**
MVDR (unit gain in look direction)	$c_0^H v(\phi_s) = 1$	$\alpha = \left[v^H(\phi_s)R_{i+n}^{-i}v(\phi_s)\right]^{-1}$
Unit noise gain	$c_0^H c_0 = 1$	$\alpha = \left[v^H(\phi_s)R_{i+n}^{-2}v(\phi_s)\right]^{-\frac{1}{2}}$
Unit gain on interference-plus-noise*	$c_0^H R_{i+n} c_0 = 1$	$\alpha = \left[v^H(\phi_s)R_{i+n}^{-i}v(\phi_s)\right]^{-\frac{1}{2}}$

* This normalization is commonly referred to as the adaptive matched filter normalization. Its use is primarily for detection purposes. Since the output level of the interference-plus-noise has a set power of unity, a constant detection threshold can be used for all angles.

The optimum beamformer passes signals impinging on the array from angle ϕ_s while rejecting significant energy (interference) from all other angles. This beamformer can be thought of as an optimum spatial matched filter since it provides maximum interference rejection, while matching the response of signals impinging on the array from a direction $\phi_{s.}$ The optimal weights balance the rejection of interference with the thermal noise gain so that the output thermal noise does not cause a reduction in the output SINR.

The optimum beamformer maximizes the SINR given by (3.17) which is, independent of the normalization. Another useful metric is a measure of the performance relative to the interference-free case, that is, x(n)= s(n)+w(n). To gauge the performance of the beam former independently of the desired signal power, the SINR is normalized by the hypothetical array output SNR, had there been no interference present, which from (3.23) is $SNR_0 = \frac{M\sigma_s^2}{\sigma_u^2}$. The resulting measure is known as the SINR loss, which for the optimum beamformer by substituting into (3.17) is

$$\mathrm{L}_{\mathrm{sinr}}(\phi_s) \stackrel{\Delta}{=} \frac{SINR_{out}(\phi_s)}{SNR_0} = \sigma_u^2 v^H(\phi_s) R_{i+n}^{-1} v(\phi_s) \tag{3.23}$$

The SINR loss is always between 0 and 1, taking on the maximum value when the performance is equal to the interference-free-case. Typically, the SINR loss is computed across all angles for a given interference scenario. In this sense, the SINR loss of the optimum beamformer provides a measure of the residual interference remaining following optimum processing and informs us of our loss in performance due to the presence of interference. It can be noticed that (3.23) is the reciprocal of the minimum-variance power spectrum of the interference plus noise.

3.2.2 Tapered Optimum Beamforming

In the derivation of the optimum beamformer, the vector v (ϕ_s) is used that was matched to the array response of a desired signal arriving from an angle ϕ_s. The resulting beamformer weight vector c_0 has unity gain in this direction, that is, $c_0^H v(\phi_s) = 1$ owing to the normalization of the weights. However, the sidelobes of the beamformer are still at the same levels as the spatial matched filter (non-adaptive beamformer), although with a different structure, as can be seen from a sample beampattern of the optimum beamformer shown in Figure 3.3.

The optimum beamformer uses the interference-plus-noise correlation matrix R_{i+n}. Now, although the beamformer weights must be estimated from intervals of the data that contain only interference (no desired signal present), they are presumably applied to segments that contain both interference and a desired signal. A desired signal at an angle (ϕ_1) may be easily found by using an adaptive beamformer directed to this angle $(\phi_s = \phi_1)$, assuming the signal strength after beamforming is significantly larger than the sensor thermal noise. However, other angles are found for potential desired signals. If one of these other angles is taken, say, $(\phi_2 = \phi_1)$, it is avoided concluding a signal is present when it may actually be due to sidelobe leakage of the signal at ϕ_1. This problem is illustrated by using the beampattern of an optimum beamformer with an interferer at $\phi = 20°$ in Figure 3.3.

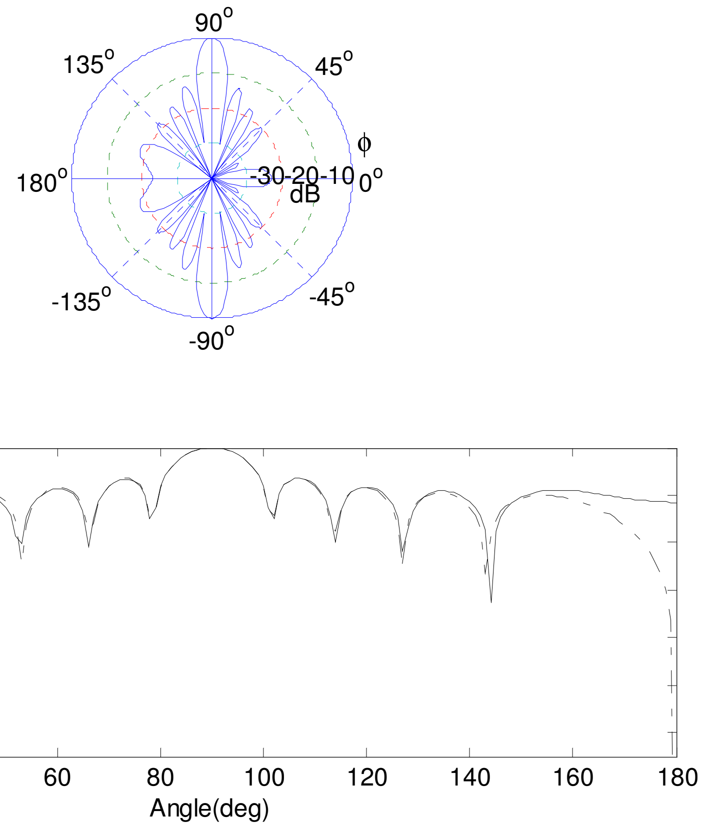

Figure 3.3: Beam pattern of the optimum beamformer when an interferer is present at an angle 20^{o} with INR=70 dB. Solid line is the optimum beamformer and dashed line is for the conventional beamformer.

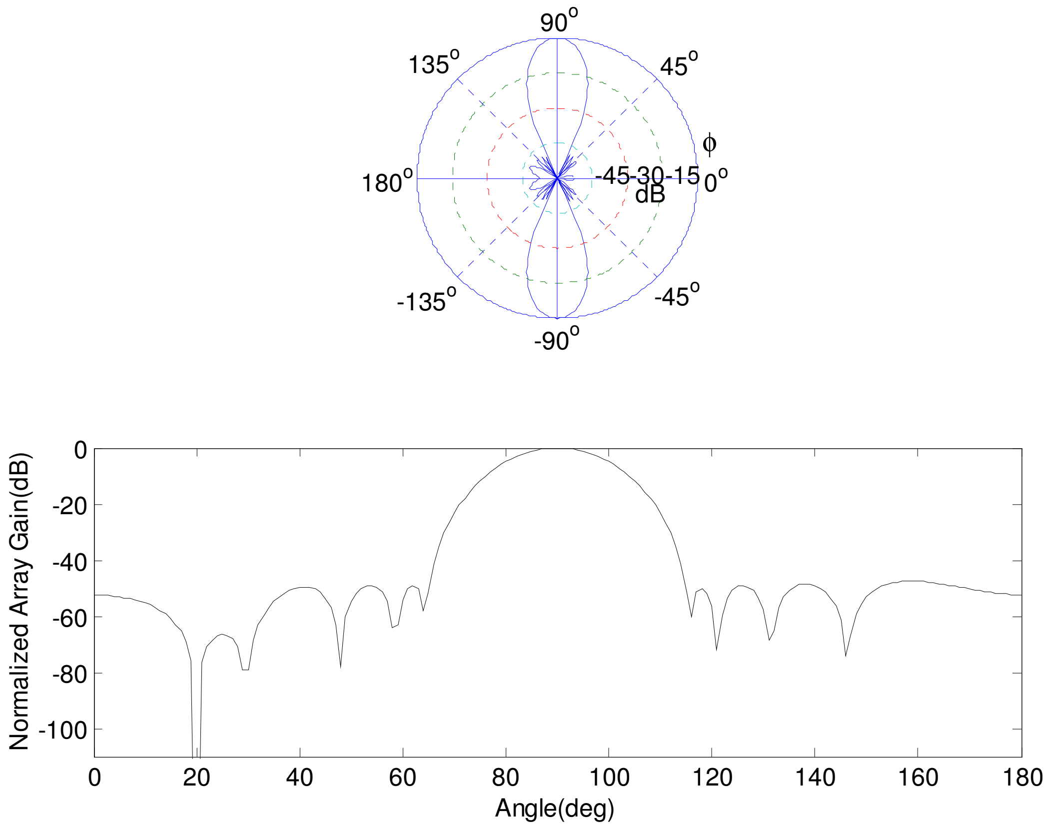

Figure 3.4: Tapered optimum beamformer (-50 dB taper)

The optimum beamformer is steered to an angle $\phi_s = 90°$. Let us assume another signal is present at $\phi_1 = 120°$ that was not part of the interference (not accounted for in the interference correlation matrix). The gain of the optimum beamformer at $\phi = 120°$ is approximately –20dB. If the strength of this signal is significantly greater than 20 dB, the optimum beamformer steered to $\phi_s = 90°$ will pass this sidelobe signal with sufficient strength that it can be erroneously concluded a signal is present at $\phi_s = 90°$. This problem is commonly referred to as a sidelobe target or desired signal problem.

The sidelobe signal problem described above can be cured, at least partially, by reducing the sidelobe levels of the beamformer to levels that sufficiently reject these sidelobe signals. As described in Section 3.1, the application of a taper to a spatial matched filter resulted in a low sidelobe beampattern. The same principle applies to the optimum beamformer [3]. A tapered array response vector at an angle ϕ_s is

$$v_t(\phi_s) = c_{tbf}(\phi_s) = t \Theta c_{mf}(\phi_s) \tag{3.24}$$

where t is the tapering vector and Θ is the Hadamard or element-by-element product. The tapering vector is normalized such that $v_t^H(\phi_s)v_t(\phi_s) = 1$ as in (3.3). The resulting low sidelobe adaptive beamformer is given by substituting in $v_t(\phi_s)$ for $v(\phi_s)$ in (3.20)

$$C_{to} = \frac{R_{i+n}^{-1} v_t(\phi_s)}{v_t^H(\phi_s) R_{i+n}^{-1} v_t(\phi_s)} \tag{3.25}$$

Dolph-Chebyshev taper is used for illustration purposes because this choice of taper provides a uniform sidelobe level. Consider the optimum beamformer with an interferer at $\phi = 20°$ from Figure 3.3 with a potential signal leaking through the sidelobe at $\phi = 120°$. If instead a tapered optimum beamformer is considered from (3.4) with a -50dB sidelobe taper, a potential signal at $\phi = 120°$ receives a -50dB level of attenuation. Figure 3.4 shows the beampattern of this tapered optimum beamformer. The sidelobe levels are significantly reduced while the null on the interferer at $\phi = 20°$ has been maintained.

The adaptive beamformer given by (3.25) is no longer optimal in any sense (unless it were somehow possible for our desired signal to be spatially matched to $v_t(\phi_s)$). However, the resulting adaptive beamformer still provides rejection of unwanted interferers via spatial nulling through the use of R_{i+n}^{-1} in (3.25). In addition, the low sidelobe levels of the beampattern reject signals not contained in the interference that are present at angles other than the angle of look ϕ_s. The penalty to be paid for the robustness provided by these low sidelobes is a small tapering loss in the direction of the look ϕ_s, given by

$$L_{taper} = c_{to}^H v(\phi_s)^2 = \left| \frac{v_t^H(\phi_s) R_{i+n}^{-1} v(\phi_s)}{v_t^H(\phi_s) R_{i+n}^{-1} v_t(\phi_s)} \right|^2 = \frac{\left| v^H(\phi_s) R_{i+n}^{-1} v_t(\phi_s) \right|^2}{v_t^H(\phi_s) R_{i+n}^{-2} v_t(\phi_s)} \tag{3.26}$$

and a widening of the main lobe beamwidth, as can be seen in the beampattern in Figure 3.3. This tapering loss indicates a mismatch between the true signal and the constraint in the optimum beamformer.

Chapter 4
Interference Cancellation using Adaptive Beamforming Techniques

In this chapter, the use of adaptive methods of beamforming, that are based on collected data from which the correlation matrix is estimated, is discussed. Adaptive beamforming is highly suitable for a CDMA system, because the spreading codes can be used as a reference for beamforming. There are two types of methods: block adaptive and sample-by-sample adaptive. A block adaptive implementation of the optimum beamformer uses a "block" of data to estimate the adaptive beamforming weight vector and is known as sample matrix inversion (SMI). In sample-by-sample adaptive methods the weights are updated for each new sample. The beam patterns of recursive least square (RLS) and least mean square (LMS) are examined later in this chapter.

4.1 Introduction

In the previous chapters, it could be seen that the criteria for optimum beamforming are closely correlated. Therefore, the choice of a particular criterion is not critically important in terms of performance, on the other hand, the choice of adaptive algorithms for deriving the adaptive weights is highly important in that it determines both the speed of convergence and hardware complexity required to implement the algorithm. The adaptive algorithms in this chapter are expressed in terms of discrete time. The common adaptive algorithms that have been investigated for beamforming in mobile communications include the LMS algorithm, the SMI technique and RLS algorithm. The LMS algorithm is simple to *implement but its dynamic range is quite limited. The permissible dynamic range is only 20 dB for a specific scenario. Since the received signals in a mobile radio system vary by more than 20 dB, power control is required if the LMS algorithm is to be used [11].*

The SMI approach offers a relatively fast convergence rate. In practice, the signal environment varies with time due to fading. Thus, the basestation must continually update the weight vector to adapt to the change in the channel. There are two problems in SMI: (1) Increased computation complexity that cannot be easily overcome through the use of very-large scale integration, and (2) numerical instability resulting from the use of finite precision arithmetic and the requirement of inverting a matrix.

An important feature of the RLS algorithm is that the inversion of the covariance matrix is replaced at each step by simple scalar division. This feature reduces the computation complexity while maintaining a similar performance. The convergence rate of the RLS algorithm is typically an order of magnitude faster than the LMS algorithm, provided that the signal to noise ratio is quite high. The forgotten factor is very dependent on the fading rate of the channel.

In addition to these three adaptive algorithms, other adaptive techniques have also been applied to beamforming in mobile communications to overcome the shortcomings or improve the performance of these algorithms.

4.2 Sample Matrix Inversion

The MVDR weight vector derived above in (3.20) assumes that the covariance matrix, R_{i+n}, is known, and is referred to as an optimal beamformer [18]. In practice, the covariance matrix is not known but rather must be estimated using training data. A beamformer that uses estimated statistics is called an adaptive beamformer. Our interest in this dissertation is in adaptive beamformers. The standard method of estimating the covariance matrix is by constructing the sample covariance matrix, given by the average of the array snapshots

$$\hat{R}_{i+n} = \frac{1}{K}\sum_{k=1}^{K} x_{i+n}(n_k)x_{i+n}^H(n_k) \tag{4.1}$$

where $x_{i+n}(n_k)$ is the k_{th} training sample, the indices n_k define the K samples of $x_{i+n}(n_k)$ for $1 \le n \le N$ and K is the total number of training samples that are available. The sample covariance matrix, $\hat{R}_{i+n}$, is the maximum likelihood estimate of the true covariance matrix, R_{i+n}. When the sample covariance matrix is used in place of the true covariance matrix in (3.20) the resulting approach is called sample matrix inversion (SMI), i.e.,

$$c_{smi} = \frac{\hat{R}_{i+n}^{-1} v(\phi_s)}{v^H(\phi_s)\hat{R}_{i+n}^{-1} v(\phi_s)} \tag{4.2}$$

and the adaptive beamformer is known as SMI adaptive beamformer. As for the optimum beamformer, an SMI adaptive beamformer can be implemented with low sidelobe control through the use of tapers. Simply, substituting a tapered steering vector from (3.24) for v (Φ_s) in (4.2)

$$c_{tsmi} = \frac{\hat{R}_{i+n}^{-1} v_t(\phi_s)}{v_t^H(\phi_s)\hat{R}_{i+n}^{-1} v_t(\phi_s)} \tag{4.3}$$

Similarly, all the adaptive processing methods, linearly constrained beamformer, all the partially adaptive beamformers, and the sidelobe canceller can be implemented in a similar fashion by substituting the appropriate sample correlation matrix for its theoretical counterpart. Of course, it is difficult to substitute an estimate $\hat{R}_{i+n}$ of the true correlation matrix R_{i+n} into the adaptive weight equation without experiencing a loss in performance. The output SINR of the adaptive beamformer is

$$\begin{aligned} SINR_{smi} &= \frac{M\sigma_s^2 \left|c_{smi}^H v(\Phi_s)\right|^2}{E\{\left|c_{smi}^H x_{i+n}(n)\right|^2\}} = \frac{M\sigma_s^2 \left|c_{smi}^H v(\Phi_s)\right|^2}{c_{smi}^H R_{i+n} c_{smi}} \\ &= M\sigma_s^2 \frac{\left[v^H(\phi_s)\hat{R}_{i+n}^{-1} v(\phi_s)\right]^2}{v^H(\phi_s)\hat{R}_{i+n}^{-1} R_{i+n}\hat{R}_{i+n}^{-1} v(\phi_s)} \end{aligned} \tag{4.4}$$

Comparing this to the SINR obtained with the optimum beamformer from (3.14), the loss associated with the SMI adaptive beamformer

$$L_{smi} = \frac{SINR_{smi}}{SINR_o} = \frac{\left[v^H(\phi_s)\hat{R}_{i+n}^{-1} v(\phi_s)\right]^2}{[v^H(\phi_s)\hat{R}_{i+n}^{-1} R_{i+n}\hat{R}_{i+n}^{-1} v(\phi_s)][v^H(\phi_s) R_{i+n}^{-1} v(\phi_s)]} \tag{4.5}$$

This SMI loss is dependent on the array data used to compute $\hat{R}_{i+n}$, which implies that L_{smi}, like the data is a random variable. This loss is also called normalized SINR. In fact, L_{smi} follows a beta distribution given by

$$p_{\beta}(L_{smi}) = \frac{K!}{(M-2)!(K+1-M)!}(1-L_{smi})^{M-2}(L_{smi})^{K+1-M} \tag{4.6}$$

Assuming a complex Guassian distribution for the sensor thermal noise and the interference signals. Here M is the number of sensors in the array, and K is the number of snapshots used to estimate R_{i+n}. Taking the expectation of the loss yields

$$E[L_{smi}] = \frac{K+2-M}{K+1} \tag{4.7}$$

Which can be used to determine the sample support required to limit the losses due to correlation matrix estimation to a level considered acceptable. From (4.7) it can be deduced that the SMI loss will be approximately –1 dB for K=5M.

4.2.1 Performance Metrics

In this section, four metrics commonly used for evaluating beamformer performance are defined.

- Signal-to-interference-plus-noise ratio (SINR)
- Normalized SINR
- Array gain (AG)
- Mean square error (MSE)

Unless otherwise stated these quantities are computed at the output of the array beamformer. A simulation example is provided to illustrate the behavior of these metrics in a more complex environment. SINR is a generalization of SNR that explicitly takes into account the impact of interference, i.e., jamming. Maximizing SINR is the optimal criterion for most detection and estimation problems. Under the assumptions of Gaussian interference and known statistics it is shown that maximizing the SINR leads to maximizing the probability of detection. SINR can be computed either at the input to the array (i.e., element level) or at the output of the array. SINR at the output of the array is taken always and therefore when SINR is not further specified it is assumed that it is output SINR.

Normalized SINR (L_{smi}) is the ratio of the SINR for a given weight vector to the SINR for the optimal weight vector. Normalized SINR is an important metric because there are classic theoretical results that have been derived using this metric.

Array gain is the third metric of interest. Array gain is the ratio of the SINR at the output of the array to the SINR at the input of the array . It is a measure of the productivity of the array and also directly impacts system detection performance. As it is shown when the performance metrics below are simulated, the value of array gain can grow quite large as it reflects not only the coherent gain from the number of elements but also the impact of nulling jammers.

The last metric of interest is mean square error (MSE). Mean square error is a measure of an adaptive filter's ability to cancel interference. As it is shown below, MSE is the most fundamental of the four metrics. Each of the other three metrics is inversely proportional to MSE under the conditions cited at the beginning of this section.

4.2.2 Performance Metric Derivation

Let us begin by defining mean square error since this quantity will appear frequently in subsequent derivations. MSE is a measure of an adaptive filter's ability to cancel interference. MSE is defined as [3]

$$MSE = E[(c.x_{i+n})^2] = c^H R_{i+n} c \tag{4.8}$$

Input SINR, or element-level SINR, is ratio of the signal power to the interference plus noise power at the individual element

$$SINR_{input} = \frac{\sigma_s^2}{\sigma_i^2 + \sigma_n^2} = \frac{\sigma_s^2}{\sigma_{i+n}^2} \tag{4.9}$$

where $\sigma_s^2, \sigma_i^2, \sigma_n^2$ are signal, interference, and thermal noise powers at the individual element level, and σ_{i+n}^2 is the interference-plus-noise power at the element-level. A convenient means of computing σ_{i+n}^2 is

$$\sigma_{i+n}^2 = \frac{1}{N} trace(R_{i+n}) \tag{4.10}$$

where N is the number of elements and $trace(R_{i+n}) = \sum_{i=i}^{N} r_{i+n}(i,i)$ .Output SINR is the ratio of the signal power to the interference-plus-noise power at the output of the array

$$SINR_{output} = \frac{(c^H x_s)^2}{E\{c^H x_{i+n}\}^2} = \frac{\sigma_s^2 (c^H v(\Phi_s))^2}{c^H R_{i+n} c} \tag{4.11}$$

Next it can be recalled from the distortion less constraint defined in table (3.1) that $c^H v(\phi_s) = 1$. This constraint implies that there is no steering vector mismatch, i.e., the steering vector used to compute 'c' is identical to the steering vector used to evaluate the SINR. Therefore, output SINR is

$$SINR_{output} = \frac{M\sigma_s^2}{c^H R_{i+n} c} \tag{4.12}$$

Lastly, it can be noted that the denominator in (4.12) is the same as the mean square error defined in (4.8). Substituting (4.8) into (4.12) yields the final expression for the output SINR. Thus it is seen that the output SINR is inversely proportional to the MSE, i.e.,

$$SINR_{output} = \frac{\alpha}{MSE} \tag{4.13}$$

The next performance measure is normalized SINR, which is defined as follows

$$\rho = \frac{SINR}{SINR_{opt}} \tag{4.14}$$

where SINR is the output SINR for a given weight vector (e.g., computed using an estimated covariance matrix), and $SINR_{opt}$ is the optimal output SINR (i.e., computed using the true covariance matrix). Substituting (4.13) into (4.14) yields

$$\rho = \frac{MSE_{opt}}{MSE} = \frac{MMSE}{MSE} \tag{4.15}$$

where the optimal MSE is more commonly referred to as the minimum MSE (MMSE). It is also noted that the MMSE will be a fixed quantity for a given scenario while the MSE will vary for each weight vector being evaluated. Therefore (4.15) can also be expressed as in order to emphasize the inverse relationship with MSE.

$$\rho = \frac{\alpha}{MSE} \tag{4.16}$$

The final performance metric of interest is the array gain (AG). Array gain is defined as follows

$$AG = \frac{SINR_{out}}{SINR_{in}} \tag{4.17}$$

Substituting (4.9) and (4.13) into (4.17)

$$AG = \frac{M\sigma_s^2}{MSE} \tag{4.18}$$

The constants in the numerator can also be replaced by a single generic constant in order to emphasize the inverse relationship with MSE, i.e.,

$$AG = \frac{\alpha}{MSE} \tag{4.19}$$

4.2.3 Performance Metric Simulation Example

In this section simulation example is presented to demonstrate the four different performance metrics defined above: mean square error (MSE), output signal-to interference-plus-noise ratio (SINR), normalized SINR, and array gain (AG). A 16 element uniform linear array with 5 noise jammers at [-64.7 -24.8 -17.4 43.3 34.5] degrees. However, for this example element-level jammer-to-noise ratio (JNR) of each jammer is varied from -7 to 53 dB. Thus the total JNR for the five jammers varies from 0 to 60 dB. All individual JNRs are the same during a given trial. An element level SNR=0 dB is used, and the thermal noise power is normalized to unity. The performance of three different beamformers: uniform weighting, *Chebychev weighting with -40 dB sidelobes, MVDR-SMI with K = 2N = 32 samples is analyzed. 1000 Monte Carlo trials are done where each realization is for a different random draw of training data. Figure 4.1 shows the MSE performance for the three different beamformers. It can be seen that, as the level of jamming increases the performance of uniform weighting quickly degrades.*

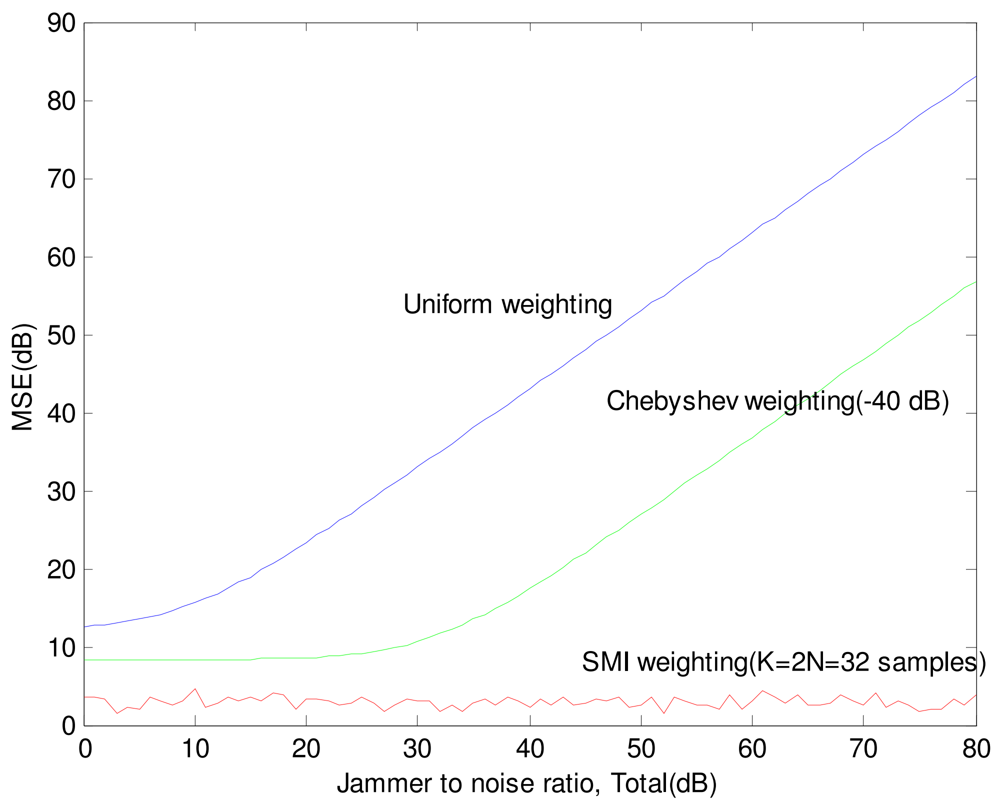

Figure 4.1: Investigation of mean square error for three beamformers: N=16 element ULA, 5 noise jammers, 1000 trials

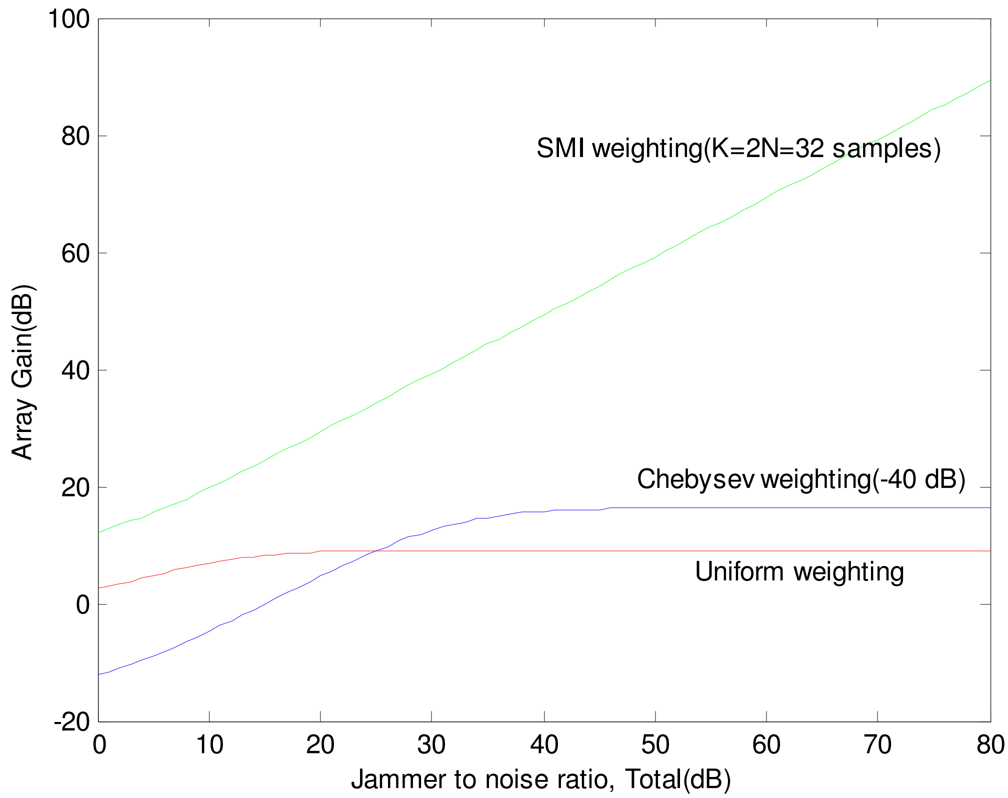

Figure 4.2: Investigation of Array Gain for Four Beamformers: N=16 element ULA, 5 noise jammers, 1000 trials.

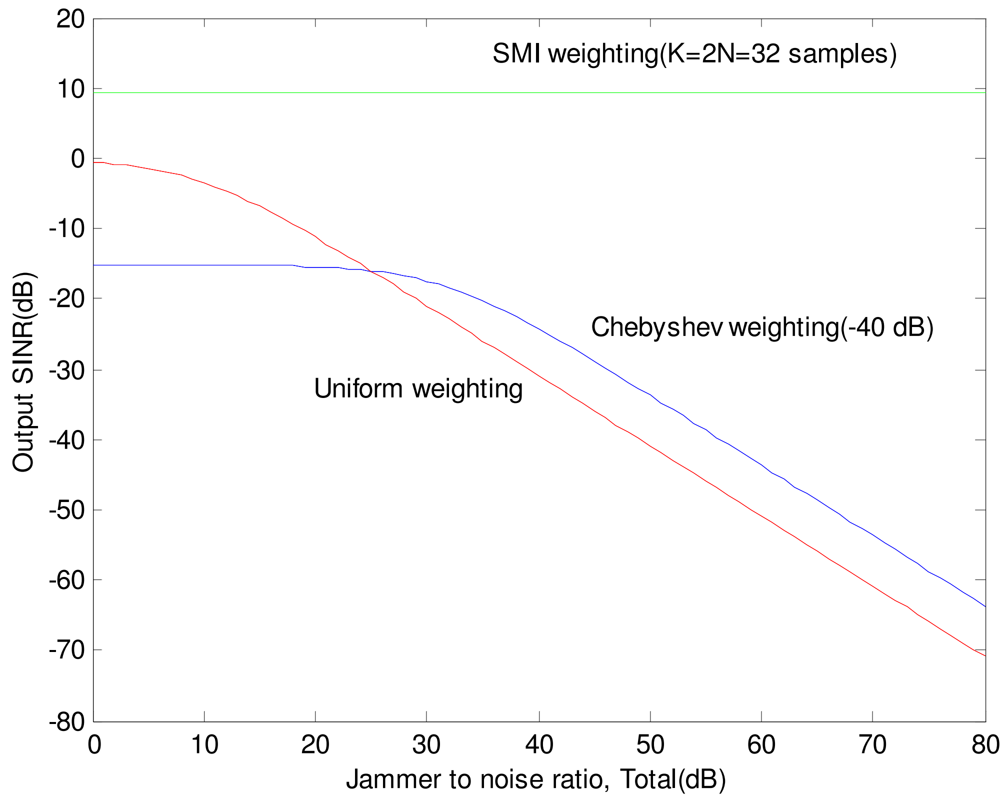

Figure 4.3: Investigation of output SINR for Four Beamformers: N=16 element ULA, 5 noise jammers, 1000 trials.

The uniformly weighted beamformer is, as expected, the worst of the three beamformers in scenarios with any appreciable level of jamming. The Chebychev beamformer performs significantly better than the uniformly weighted beamformer due to its much lower (-40 dB) sidelobe levels. The Chebychev performance, however, begins to degrade when the JNR level increases above about 28 dB. The reason that the degradation occurs around 28 dB as opposed to around 40 dB is because jamming, unlike noise, adds coherently across the array. There are 16 elements, which, unfortunately, provide 12 dB of coherent gain for the jammers.

The next beamformer is the MVDR-SMI beamformer with K = 2N = 32 training samples. This beamformer adaptively nulls each of the jammers, as in figure 4.1, and thus provides performance that is independent of the jammer-to-noise ratio. Overall the performance of this beamformer is quite good. Next the array gain metric is examined in figure 4.2. As the JNR level increases the array gain values for each of the beamformers increase in recognition of the fact that the jammers are being suppressed. For the classical beamformers (uniform weighting and Chebychev weighting) there is a limit to the amount of array gain dictated by the level of the beampattern sidelobes.

The adaptive beamformers, MVDR-SMI is able to null the jammers all of the way down to the noise floor. Thus it achieves an array gain that is equal to the total JNR plus the coherent gain from N elements. For example, with N = 16 elements (12 dB) and a JNR of 60 dB, a total array gain of 72 dB is possible. The MVDR-SMI beamformer approach this level of array gain. This shows the benefit of adaptive jammer nulling as opposed to deterministic sidelobes.

The next metric, output SINR is plotted in Figure 4.3. This is simply an inverted and scaled version of the MSE plot shown in Figure 4.1. It can be seen that at low JNR levels the beamformer results are clustered around 12 dB. The element-level SNR is 0 dB in this example and there are 16 elements. Thus 12 dB is the value of output SINR that would be expected. As the jammer-to-noise-ratio increases the classical beamformers each reach a threshold where SINR performance begins to degrade. The adaptive beamformers provide jammer nulling throughout and thus are able to maintain the peak level of SINR.

The last performance metric, normalized SINR, is shown in Figure 4.4. Being a normalized version of output SINR the only difference between Figures 4.3 and 4.4 is the y-axis scaling.

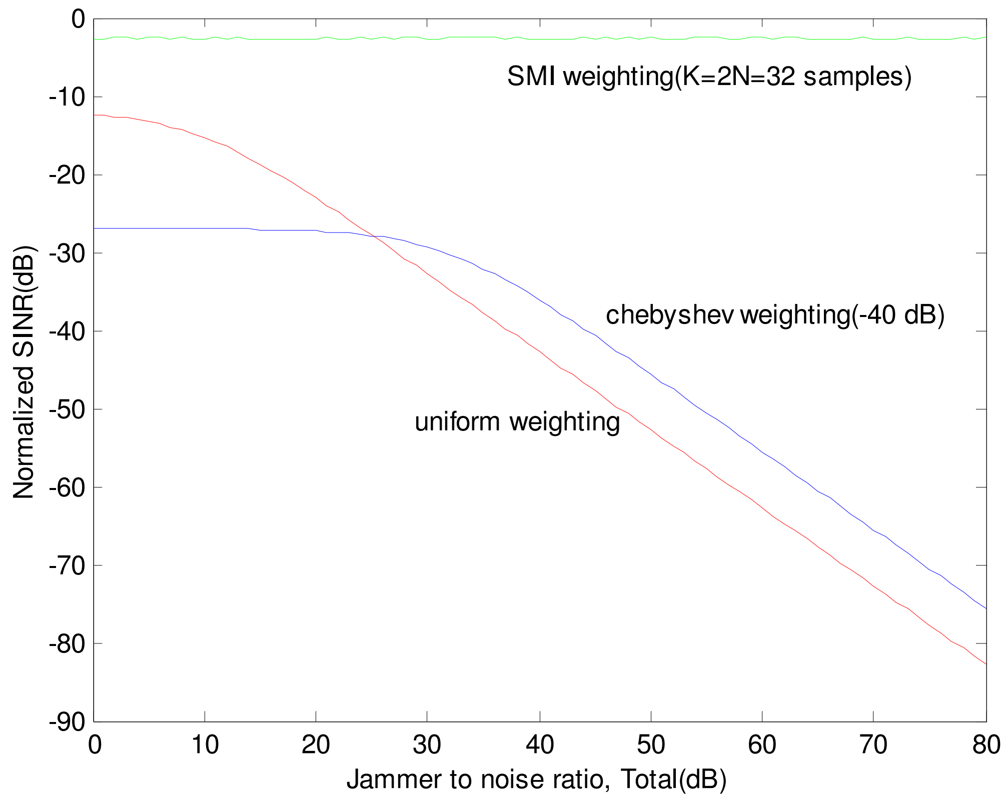

Figure 4.4: Investigation of normalized SINR for three beamformers: N=16 element ULA, 5 noise jammers, 1000 trials.

4.2.4 Monte Carlo Simulation of SMI beamformer

In this section, the use of Monte Carlo simulation is demonstrated using spatial array processing and the SMI beamformer introduced in above section. This example is taken because an analytical solution exists that characterizes the normalized SINR ρ as a function of the number of training samples.

The adaptive array architecture that is simulated is shown in Figure 4.5. The randomness for this system comes from two sources. Each of the M elements has its own receiver, and each receiver contributes thermal noise to the system. The impact of these receivers noise sources is characterized by a diagonal covariance matrix, $R_n = \sigma_n^2 I$. Additionally there is “colored noise" in the system due to the presence of multiple barrage jammers, also called interferers. Each jammer is modeled as Gaussian random processes and is characterized by the following covariance matrix [3]

$$R_i = \sigma_i^2 v(\Phi_i) v^H(\Phi_i) \tag{4.20}$$

Where σ_i^2 is the jammer's power and $v(\Phi_i)$ is the array manifold vector associated with the jammer's direction of arrival, Φ_i. Formation of the overall interference-plus-noise covariance matrix, $R_{i+n} = R_i + R_n$ is an important early step in the simulation. Next, Figure 4.6 shows the basic approach used for the simulation.

The simulation is divided up into three sections: definitions and initializations, main program, and outputs. Within the main program there are three main functions: generating the training data, computing the adaptive weight vector, and evaluating the performance of the adaptive weight vector. A key part of the definitions and initializations stage involves forming the true interference-plus-noise covariance matrix, R_{i+n} as was discussed above. The adaptive algorithms are based on training data snapshots drawn from R_{i+n}. Thus a key function at the start of the main program is generating data snapshots. These snapshots can be computed as follows

$$x_i(n_k) = R_{i,n}^{1/2} a_k \tag{4.21}$$

where

$$a_k = \frac{1}{\sqrt{2}}(randn(N,1) + j \times randn(N,1)) \tag{4.22}$$

where “ randn” refers to MATLAB’s normally distributed random number generator and $j = \sqrt{-1}$. Observe that

$$E[a_k a_k^H] = I \tag{4.23}$$

And therefore,

$$E[x_k x_k^H] = R_{i,n}^{1/2} E[a_k a_k^H] R_{i,n}^{1/2} \tag{4.24}$$

$$= R_{i,n}^{1/2} I R_{i,n}^{1/2} \tag{4.25}$$

$$= R_{i,n} \tag{4.26}$$

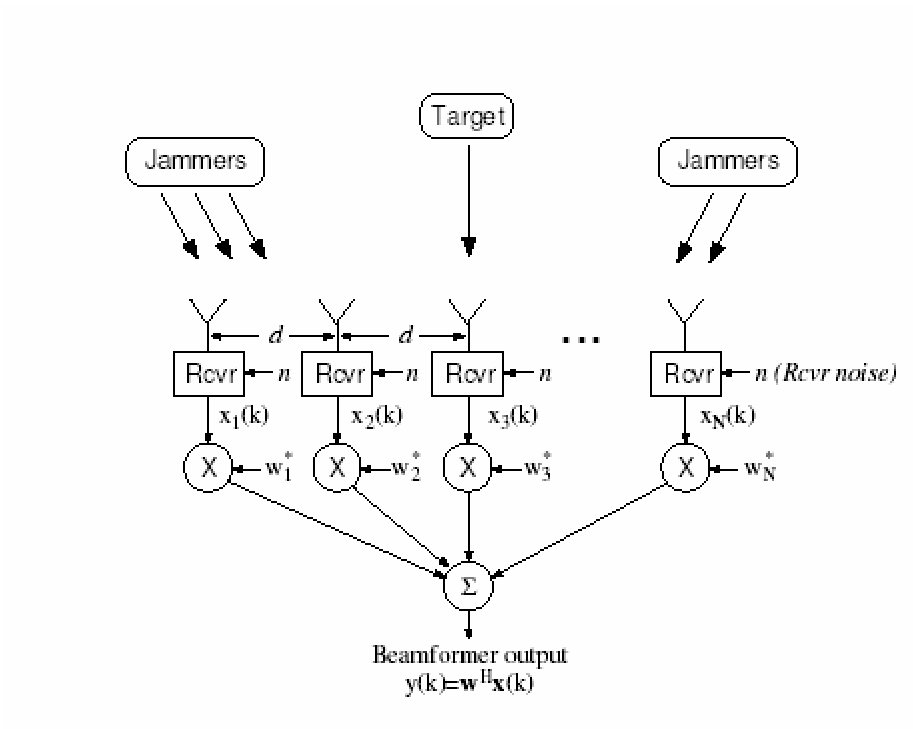

Figure 4.5: Block Diagram of an Adaptive Array

In figure 4.5, $x_i(k)$ is the kth measurement taken at element i, w_i^* is the complex conjugate of the i_{th} complex weight, y is the beamformer output, and N is the number of elements.

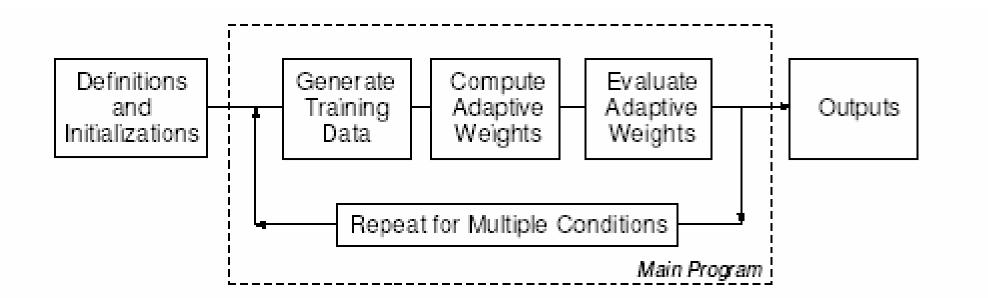

Figure 4.6: Basic Approach to Monte Carlo Simulation for Adaptive Arrays.

The second main function within the main program is computing the adaptive weight vector. In this section the MVDR-SMI beamformer is evaluated, which as in (4.2) is computed from

$$c_{smi} = \frac{\hat{R}_{i+n}^{-1} v(\phi_s)}{v^H(\phi_s)\hat{R}_{i+n}^{-1} v(\phi_s)} \tag{4.27}$$

where $\hat{R}_{i+n} = \frac{1}{K}\sum_{k=1}^{K} x_{i+n}(n_k) x_{i+n}^H(n_k)$ is the sample covariance matrix computed from the training snapshots, $x_{i+n}(n_k)$.

The third main function of the main program is evaluating the adaptive weight vector's performance. Section 4.4 provides a detailed discussion of four different metrics. Normalized SINR is used in this section. Normalized SINR, ρ, is a random variable that has a beta distribution. Monte Carlo simulation is used to compute the sample mean, $\overline{\rho}$, of this random variable, i.e.,

$$\overline{\rho} = \frac{1}{N_{mc}} \sum_{n=1}^{N_{mc}} \hat{\rho} \tag{4.28}$$

Where $\hat{\rho}$ is the normalized SINR computed on a single trial, and N_{mc} is the total number of Monte Carlo trials. Recall from Section 4.4 that

$$\rho = \frac{MMSE}{MSE} = \frac{\alpha}{MSE} \tag{4.29}$$

There is an important caution with regard to (4.29). When evaluating the sample mean, $\overline{\rho}$, one must compute $\hat{\rho}$ for each trial and then literally apply (4.28). Next the MVDR-SMI simulation is implemented. The simulation parameters are the same as those used above in the simulation of Section 4.4, except that now instead of varying the jammer-to-noise ratio, the JNR is fixed at 50 dB per jammer, and vary the number of training samples. The results of the simulation are shown in Figure 4.7. Note how poorly the MVDR-SMI beamformer does when limited to only K = 1N = 16 samples. Recall from (4.7) that the analytical solution for the MVDR-SMI normalized SINR is given by

$$E[L_{smi}] = \frac{K + 2 - M}{K + 1} \tag{4.30}$$

Where M is the number of elements and K is the number of training samples. An excellent agreement is seen between the simulated and the analytical solutions. Thus, Monte Carlo simulation is an important source for the validation of codes.

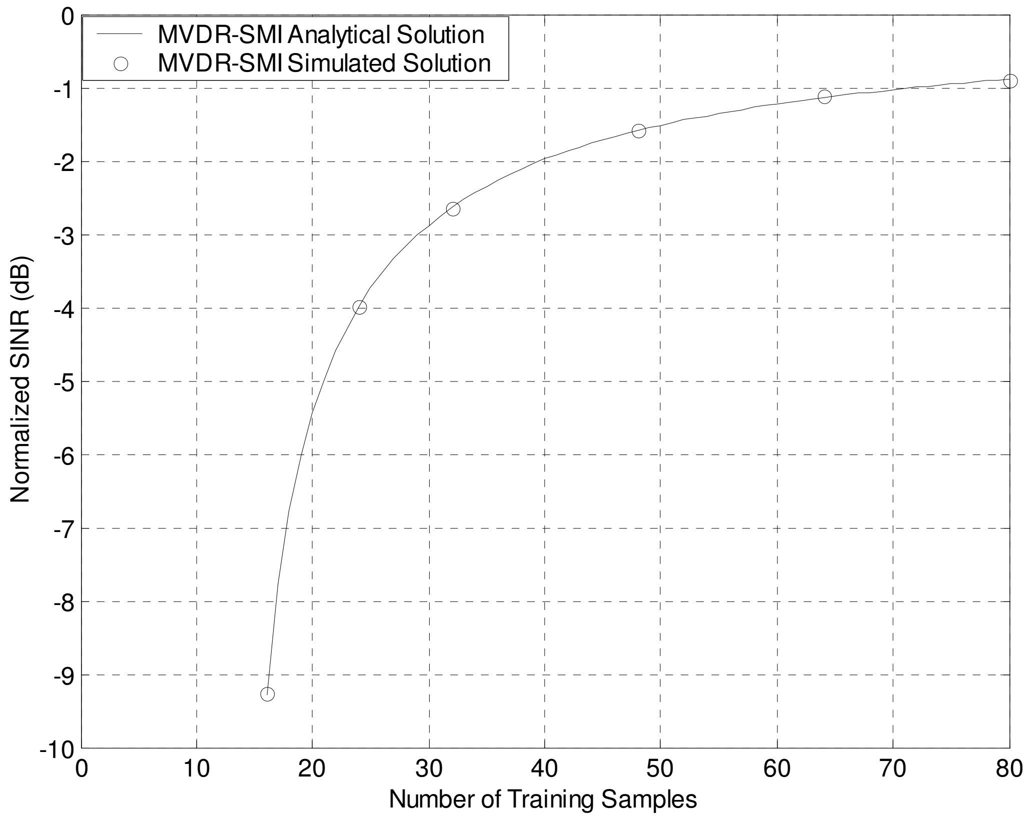

Figure 4.7: Validation Example for Monte Carlo Simulation. Comparison of Analytical and Simulated Solutions for the Normalized SINR of an MVDR-SMI Beamformer:1000 Monte Carlo trials.

4.3 Least Mean Squares Algorithm

The most common adaptive algorithm for continuous adaptation is the least-mean-square (LMS) algorithm. It has been well studied and well understood. It is based on the steepest-descent-method, a well-known optimization method, that recursively computes and updates the weight vector. It is intuitively reasonable that the successive corrections to the weight vector in the direction of the negative of the gradient vector should eventually lead to the MSE, at which point the weight vector assumes its optimum value. According to the steepest-descent *method, the updated value of the weight vector at time n+1 is computed by using the simple recursive relation [8]*

$$w(n+1) = w(n) + \frac{1}{2}\mu[-\nabla(E\{\varepsilon^2(n)\})] \qquad \text{or} \qquad w(n+1) = w(n) + \mu[r - Rw(n)] \quad (4.31)$$

Where **R** is covariance matrix and **r** is cross correlation matrix between the desired signal and incoming signal. In reality, an exact measurement of the gradient vector is not possible, since this would require a prior knowledge of both R and r. the most obvious strategy is to use their instantaneous estimates, which are defined, respectively, as

$$\hat{R}(n) = x(n)x^H(n) \text{ and } \hat{r}(n) = d(n)x(n) \quad (4.32)$$

The weights can be updated as

$$\hat{w}(n+1) = \hat{w}(n) + \mu x(n)[d(n) - x^H(n)\hat{w}(n)] = \hat{w}(n) + \mu x(n)\varepsilon(n) \quad (4.33)$$

The gain constant μ controls convergence characteristics of the random vector sequence w(n). This is a continuously adaptive approach, where the weights are updated as the data are sampled such that the resulting weight vector sequence converges to the optimum solution. Continuous adaptation works well when statistics related to the signal environment are stationary. The primary virtue of the LMS algorithm is its simplicity. Its performance is acceptable in many applications. However, its convergence characteristics depend on the eigen structure of R. When the eigen values are widely spread, convergence can be slow and other adaptive algorithms with better convergence rates should be considered. The beamforming using LMS algorithm is shown in fig. 4.8. The gain control parameter μ is taken to be .0013. In this example, the signal is assumed to be coming from 0^o with SNR=10 dB and two interferers from -20^o and 50^o respectively both with SIR=-10 dB.

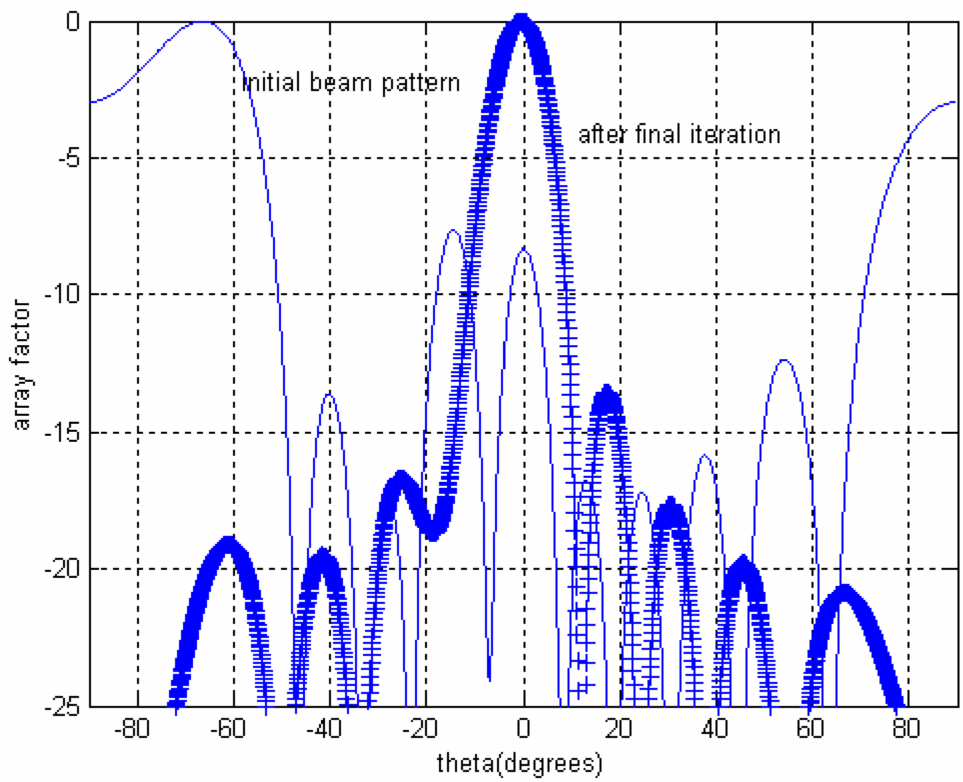

Figure 4.8: Beam pattern of a LMS adaptive beamformer for μ=. 0013, No. of antenna elements N=10, No. Of interferers = 2, SIR=[-10 –10], SNR=10,Angle of arrival of interferers = [-20 50], Angle of arrival of signal = 0 degree, No. of iterations=1000.

4.4 Recursive Least Square Algorithm

In RLS algorithm, **R** and **r** can be estimated using the weighted sum [8]

$$\tilde{R}(n) = \sum_{i=1}^{N} \gamma^{n-i} x(i) x^H(i) \quad \text{and} \quad \tilde{r}(n) = \sum_{n=1}^{N} \gamma^{n-i} d(i) x(i) \tag{4.34}$$

The weighting factor, $0 \le \gamma \le 1$, is intended to ensure that data in the distant past are "forgotten" in order to allow the processor to follow the statistical variations of the observable data. Factoring out the terms corresponding to i = n in (4.34), we have the following recursion for updating both $\tilde{R}(n)$ and $\tilde{r}(n)$

$$\tilde{R}(n) = \gamma \tilde{R}(n-1) + x(n) x^H(n) \quad \text{and} \quad \tilde{r}(n) = \gamma \tilde{r}(n-1) + d(n) x(n) \tag{4.35}$$

Using Woodbury's identity, the following recursive equation is obtained for deriving the inverse of the covariance matrix,

$$R^{-1}(n) = \gamma^{-1}[R^{-1}(n-1) - q(n)x(n)R^{-1}(n-1)] \tag{4.36}$$

Where the gain vector q(n) is given by

$$q(n) = \frac{\gamma^{-1}R^{-1}(n-1)x(n)}{1+\gamma^{-1}x^H(n)R^{-1}(n-1)x(n)} \tag{4.37}$$

To develop the recursive equation for updating the least square estimate $\hat{w}(n)$,

$$\begin{aligned} \hat{w}(n) &= R^{-1}(n)r(n) \\ &= \gamma^{-1}[R^{-1}(n-1) - q(n)x(n)R^{-1}(n-1)] \times [\gamma r(n-1) + d(n)x(n)] \end{aligned} \tag{4.38}$$

Rearranging the above equation the weight vector can be updated as follows:

$$\hat{w}(n) = \hat{w}(n-1) + q(n)[d(n) - \hat{w}^H(n-1)x(n)] \tag{4.39}$$

An important feature of the RLS algorithm is that the inversion of the covariance matrix is replaced by a simple scalar division. The convergence rate of the RLS algorithm is typically an order of magnitude faster than that of the LMS algorithm, provided that the signal-to-noise ratio is high. An example of beamforming using RLS algorithm is shown in fig.4.9. The RLS algorithm is used for updating the weight vector for an antenna array with number of elements N=10. The forgetting factor is taken to be 0.95. The converged weights are then multiplied with steering vector steered to the direction of arrival of incoming signal i.e. 45^o to plot the beam pattern.

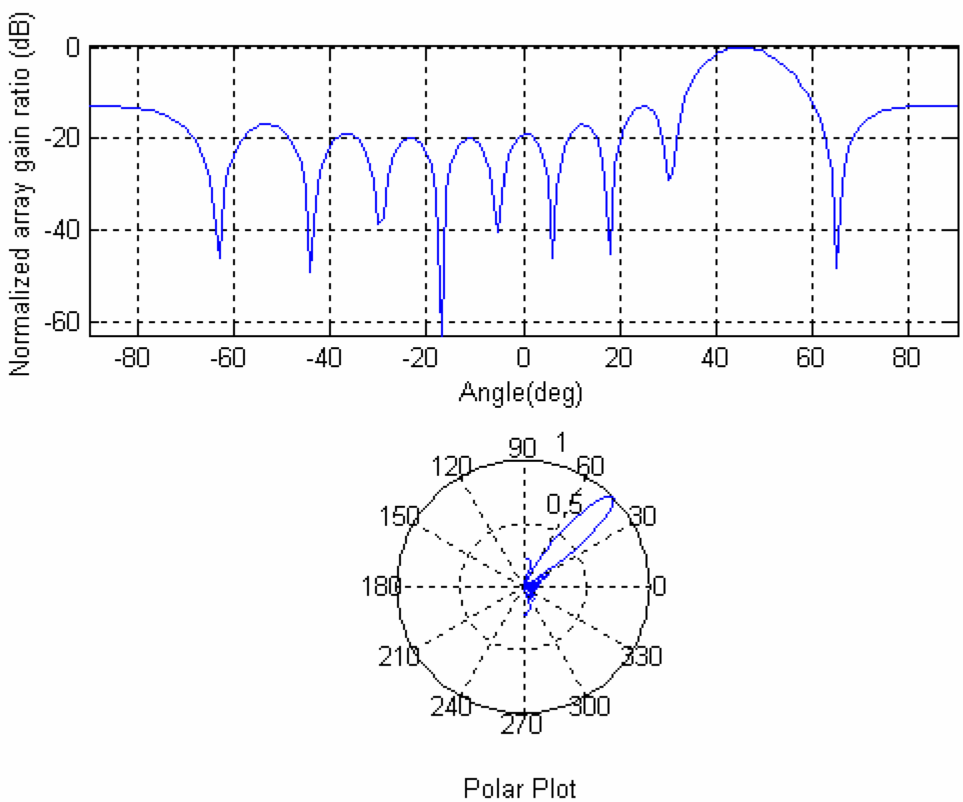

Figure 4.9: Beam pattern of a RLS adaptive beamformer for γ = .95, No. of antenna elements N=10, Angle of arrival of signal = 45 degree, No. of iterations=100.

Chapter 5

Tapered Beamforming Technique for Antenna Arrays

In this chapter, a novel two-step tapered beamforming algorithm is described for flexible sidelobe adjustment. In the mobile communication systems like CDMA where the intra cell interferers are large in number, sidelobe adjustment would be a simple solution towards suppressing co-channel interference and hence improving CIR performance. The algorithm places a very low sidelobe level over a large width in the beam pattern. The convergence of this algorithm is fast and requires only two to three iterations. This beamforming algorithm is suitable for uplink and downlink since it is based on the DOAs estimated in uplink. The algorithm provides flexible parameter adjustment (sidelobe level, null depth, main lobe width and null width) together with very low computational effort.

5.1 Introduction

Antenna arrays reduce the co-channel interference by spatial variations of antenna gain [12]. This improves the QoS and hence the system capacity by a large margin as compared to omni-antenna at the BS of mobile communication systems. In CDMA systems as the number of co-channel interferers is very large, antenna array is going to be an integral part of the 3G systems. Owing to large number of interferers, to know the angular directions of all the interferers for a MS would be a cumbersome task, if not impossible to form the beam to null them. In the uplink, covariance matrix is estimated to find out the DOAs of the interferers of a MS and maximize the signal to interference ratio for its proper beamforming. In CDMA mobile communication systems the main criterion for beam forming is to maximize the power received from the desired direction and minimizing the average power in the undesired direction. But, due to large number of interferers in CDMA systems nulling or reducing power towards individual interferers as per their strength will not be possible, as an antenna has a limited degrees of freedom because of limited number of antenna elements. It should be noted that a receiver with M antennas could suppress M-1 interfering signals. Thus, instead of nulling the error prone non-unique directions of the interferers, an adaptive side lobe adjustment would be better. This would require a beam forming algorithm capable of shaping the overall side lobe levels rather than nulling/reducing the gain in the individual interferers direction. It should be capable of providing different side lobe level requirements with one algorithm.

The beamforming technique analyzed in this chapter is capable of obtaining a Chebyshev pattern with minimum equal side lobe level for a given main lobe beam-width and vice versa. This technique is based on iterative scheme, which calculate the weight vectors iteratively, till the power ratios assigned to the corresponding side lobes is achieved. This is a flexible and computationally efficient algorithm that can provide any desired antenna patterns. This method has an advantage that with the knowledge of many points on the pattern different types of patterns can be obtained. This pattern synthesis procedure can even be applied to antenna arrays with non-isotropic elements with arbitrary spacing. The major advantage of this synthesis procedure is its simplicity and robustness in adapting to the need.

5.2 System Model

Let us consider N isotropic element linear array with a uniform spacing (ULA), non-uniform amplitude and progressive phase excitation. According to Schelkunoff, the field due to this antenna array could be represented in a polynomial form as [1]

$$f(\Omega_m) = a_o\Omega_m^0 + a_1\Omega_m^1 + a_2\Omega_m^2 + \dots\dots\dots + a_N\Omega_m^{N-1} \qquad (5.1)$$

where

$$\Omega_m = e^{j\Psi_m}; \Psi_m = (2\pi/\lambda).d.\cos(\theta_m) + \alpha \qquad (5.2)$$

a_N is the non-uniform real amplitude, d is the inter-element spacing, λ is the wavelength of the carrier, θ_m is the angle from the axis of the array and α is the progressive phase excitation. f(Ω)

is also called Array Factor (AF). If a non-uniform phase excitation is considered, then the above polynomial could be written in terms of complex amplitude w, i.e. real amplitude with phase, as

$$f(\Omega_m) = w_o\Omega_m^0 + w_1\Omega_m^1 + w_2\Omega_m^2 + \dots\dots\dots + w_N\Omega_m^{N-1} \tag{5.3}$$

In the matrix notation equation (5.3) can be represented as

$$f(\Omega_m) = w_m^T.\Omega_m \tag{5.4}$$

This AF gives the field due to the antenna array with complex coefficients fed at each antenna element in m[th] direction. If M points are considered on the angular space in the range $[0, \pi]$, then the above equation could be denoted as

$$F_{M*1} = \Omega_{M*N}.w_{N*1}^T \tag{5.5}$$

F is the field vector, Ω is the steering vector and w is the weight vector. If symmetric excitement is considered i.e. the reference point is the center of the array, summation of phases with weights would yield real steering vectors. To obtain specific power pattern weight vector need to be calculated for particular F. Thus, if the corresponding field points are provided in the angular space, the desired beam can obtain with specified side lobe levels. In the far field, the F will be real vector denoting the magnitude of the field strength. This lead to the

$$\mathrm{Re}[F_{M*1}] = \mathrm{Re}[\Omega_{M*N}].w_{N*1}^T \tag{5.6}$$

The solution to this equation would be a set of real weights, given as

$$w = \Omega^{-1}F \tag{5.7}$$

Thus, using real weights at the antenna elements the desired beam can be formed, i.e. the appropriate levels of the main lobe and side lobes can be obtained and by applying a proper phase shift to the antenna elements the beam can be steered. The position of nulls would be determined by the width of the sidelobes. Different applications require different beamforming constraints. Some may require proper positioning of nulls in particular directions like radars while some may require lower sidelobes relative to the main lobe like mobile communications. In CDMA mobile communications where there are large number of interferers, a beamforming technique is sought that would efficiently suppress the power in the undesired direction at the same time maximizing the power in the desired direction. As the antenna array could be of only finite size, it has finite degree of freedom, i.e., only N-1 nulls can be placed for an N element antenna array. But the number of co channel mobile stations are much larger than N. Moreover to place these nulls we must know the direction of the interferers which introduces additional complexity. A beam forming technique that maximizes the power in the desired direction and minimizing the average power in the undesired direction is the main criterion required for beamforming. Hence the sidelobe levels of the antenna pattern are more important than placing the nulls. One more concern is that once a beam is formed for given sidelobe levels, it should remain constant while steering the beam by applying proper phase shift. These issues are resolved in this beamforming technique and the concepts are established through simulations.

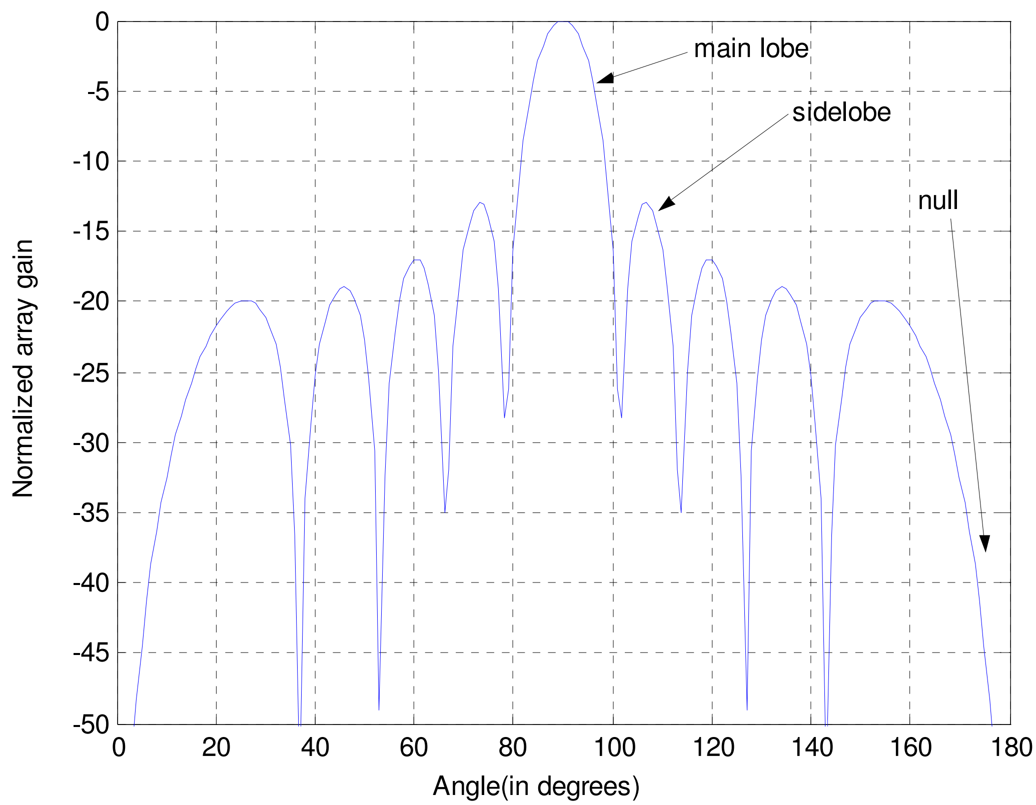

Figure 5.1: Normalized field pattern for ULA with N=10,d=$\lambda/2$,α=0

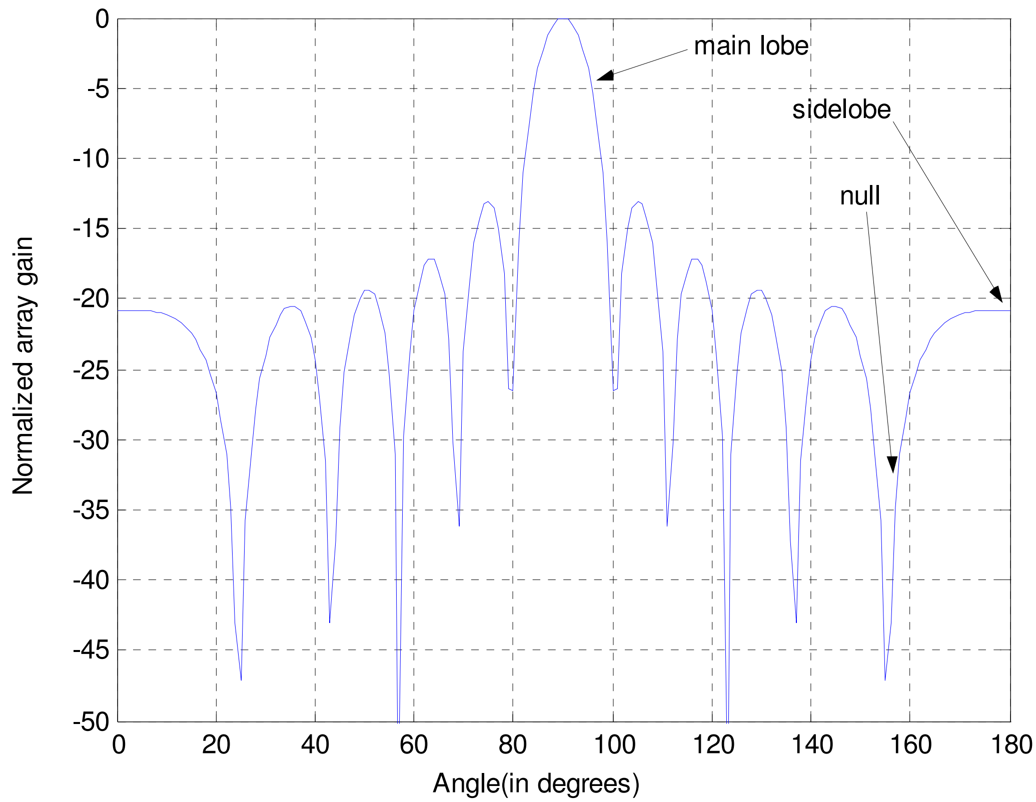

Figure 5.2: Normalized field pattern for ULA with N=11,d=λ/2,α=0

First, the nature of the field pattern of a linear array with weight vector equal to unity i.e. a uniformly excited linear array (ULA) is considered. The inter element spacing is taken as d=λ/2. The progressive phase shift, $\alpha = 0$, i.e., it is a broadside array. The function f is plotted as

$$f(\Omega) = w^T \cdot \Omega \text{ for } 0 \le \theta \le \pi \tag{5.8}$$

From the electric field plot as per (5.8) in Fig. 5.1, it is observed that the main beam is in the broadside direction, i.e., at $\theta = \pi / 2$. The nulls are the points cutting the x-axis at f=0. Looking at the sidelobes it could be observed that they alternate in sign with reducing levels towards endfire direction, i.e., towards endfire direction, i.e., towards $\theta = 0$. This field configuration is a characteristic of the sinc function. $f(\Omega)$ in (5.8) is Geometric Progression (GP) with complex terms, which could be written as

$$f(\Omega) = \frac{\sin(N\psi / 2)}{\sin(\psi / 2)} \tag{5.9}$$

For small values of ψ, the function could be approximated as

$$f(\Omega) = \frac{\sin(N\psi/2)}{\psi/2} = N.\sin c(N\psi/2) \tag{5.10}$$

Thus field expression is a normalized sinc function and hence the nature of the field strength in the space domain is as described above. To calculate a generalized field pattern, appropriate weight vectors can be chosen for the antenna elements. This would mean that the field pattern would be weighted sum of cosine series as evident from (5.4). This enlightens the fact that the basic nature of the field pattern would resemble the sinc pattern for the main lobe region and sine or cosine pattern for the sidelobe region. Thus, peaks of the field patterns would always alternate in sign with nulls between them. Based on this conclusion, the function values of antenna pattern peaks are expressed in alternative sign in the forcing function f (Ω). Thus the elements of the vector F could be of the form

$$F = \begin{bmatrix} Mainlobe \\ -Sidelobe_1 \\ +Sidelobe_2 \\ . \\ . \\ . \\ (-1)^{n+1} Sidelobe_{N-2} \end{bmatrix} \tag{5.11}$$

Our requirement is to form the antenna beam for given sidelobe levels in specific angular space. As the total power in the beam remains constant, the required sidelobe levels could be achieved by placing the nulls properly in the angular space. Chebyshev gave a polynomial function approach to determine such position of nulls, which would give equal sidelobe levels. This would be a nice approach if we were only concerned with equal sidelobe levels. In mobile communications, at the BS, the beam formation should be able to achieve any arbitrary sidelobe levels as per the requirements. Thus a generalized and flexible technique is required to achieve this. Here, this would be achieved by formulating iterative matrix problem.

5.3 Algorithm Used

This algorithm is discussed in [14]. There was a problem in the placement of nulls in case of odd number of elements, which is solved by placing the null in the end fire direction at approximately near to 180^{o} not exactly at 180^{o}. The two-step beamforming algorithm is as follows:

$$w^{(0)} = 1$$
$$\Omega^{(0)} = \Omega_{(0)}$$
$$w^{(n+1)} = (\Omega^{(n)})^{-1}.F \tag{8}$$

Here, $\Omega_{(0)}$ is the initial steering matrix with given main beam direction and the direction of the side lobes of ULA. The basic property of beamforming is imbedded in ULA, which is exploited in knowing the side lobe directions as an initial step. Once the side lobe directions are known, depending on the relative magnitude required for the side lobes forcing vector F is formulated. The first set of weight vectors is calculated using equation (8). For inverse of Ω, matrix should be a square and for N element array, there are N-2 distinct side lobes. To make lesser computation, instead of using singular value decomposition, the matrix is made square. This could be done in two different ways depending on the number of antenna elements.

1. If the number of antenna elements is even, a null in the end fire direction could be impressed at $\theta = 0$ or $\theta = \pi$ for no-endfire array and a null at $\theta = \pi / 2$ for end fire array, to make the matrix square and vector F of length N. This is because even number of elements tends to have null in the endfire direction for broadside arrays and null at the broadside for the endfire arrays as shown in figure 1.

2. If the number of antenna elements is odd, the null nearest to the main lobe could be held constant. Another possibility could be to repeat a side lobe at the endfire direction for $\theta = 0$ and $\theta \sim= \pi$. This is because odd number of elements tends to have side lobes in the endfire direction in ULA as shown in figure 2. The pseudo inverse can now be found based on singular value decomposition.

The iterative steps required for the algorithm could be stated as follows:

1) Formulate ULA with equispaced elements with $d \leq \lambda / 2$.
2) Find the positions of the side lobes by simple peak finding (change in slope routine).

3) Formulate the matrix Ω and F.
4) Find the weight vector, w.
5) Obtain the pattern with this weight vector and find the magnitude of the side lobes.
6) Find the error between the desired F and new side lobe peaks, say F1. If F-F1 $\leq \varepsilon$ where ε is the acceptable error, then stop, else repeat step 4. In the simulations the iteration is said to converge when mean square error is minimum, i.e., $\overline{\in}^{2^{(n+1)}} - \overline{\in}^{2^{(n)}} = 0$.

5.4 Results & Conclusion

Convergence:

The convergence of the two step iterative algorithm is proved by synthesizing the Chebyshev antenna pattern, as it is the only and finest example of optimum beamforming with equal side lobe levels for a minimum beamwidth as it is based on closed form polynomial function. The algorithm is applied to ULA for different number of elements and the beampattern is finally converged to Chebyshev pattern. The ULA pattern is known to have minimum beamwidth (BW), and the finally converged beam also has minimum beamwidth for a given sidelobe level, which is similar to the Chebyshev beampattern. The comparison of BW is given in table 5.1. For N=10, starting with initial BW=21.54 for first sidelobe at 13 dB, the converged beam has a BW=22.60 for ESLL=30 dB.

Table 5.1: The initial and final beam width for different antenna elements

No. of elements	Initial Beamwidth (deg)	Converged Beamwidth (deg)
10	21.54	22.60
11	19.27	20.43
16	10.48	13.75

For number of elements, N=10, a power pattern of a broadside array is obtained with a constraint of equal side lobe levels equal to –30 dB. The initial and final patterns are shown in fig. 5.3 and fig. 5.4. To converge to the required beam, it took only three iterations. The convergence /error graph is shown in fig 5.5 for ten number of antenna elements showing the algorithm to have a fast convergence.

For odd number of elements i.e. N=11 and equal side lobe level=-30dB, the side lobes in the endfire could be spotted in fig. 5.2. the converged beam for N=11 is shown in fig. 5.6. To converge to the required beam it took only three iterations.

The initial beampattern for ULA with 20 elements is shown in fig. 5.7. In fig. 5.8 the converged beampattern is shown. The convergence speed is shown for large number of elements. It also took three iterations as shown in fig. 5.9. Similar observations were made with number of antenna elements N=16. The initial and final beam pattern is shown in fig. 5.10 and 5.11 respectively. The convergence is shown in fig. 5.12.

Flexibility: In CDMA systems, sometimes the large numbers of interferers are present in a known direction. With this algorithm very low side lobes can be obtained only in that direction and equal side lobe level maintained in other directions. The sidelobe on left and right direction of the main beam are made with ESLL=-50 dB while the other sidelobes are kept at –30dB.this is shown in fig. 5.13 and fig. 5.14. In fig. 5.15 the first sidelobe are made –50 dB while other sidelobes are having ESLL=-30dB. In fig. 5.17 the first and second sidelobe is made –50 dB while other sidelobes are having ESLL=-30dB. The fig. 5.17 shows the tapering on the outward direction.

Realizability: The major issue in design in the beamforming strategies is that current ratios of the antenna elements should be practically realizable. The beamforming using this algorithm gives very small current ratios e.g. for N=20, current ratio = 3.2 and for N=10, current ratio = 3.4 is found which are practically realizable.

Steerability: The beam can be steered in any desired direction by applying proper phase shift. For this radiation pattern of no. of antenna elements N=16, steered at an angle of 60^o and 45^o is shown in fig. 5.18 and fig. 5.19 respectively. It could be observed that by adding progressive phase shift to the elements does not disturb SLL. This is a very useful characteristic of the beamforming because this way, the SLL could be controlled by real weights and external phase control can be used to steer the beam without increasing SLL in any direction.

Capacity Improvement in WCDMA Systems: This reduction in interference power by presenting low sidelobe levels to the undesired users leads to direct and linear increase in Carrier to Interference ratio (CIR) according to (5.12) where N is the number of users in one cell, S_c is the power of any mobile unit, I_{oc} is the total interference from all the cells (first two tiers are taken), α is the voice activity factor which is taken to be 3/8.

$$CIR = \frac{1}{(N-1) + I_{oc} / \alpha S_c} \tag{5.12}$$

It is shown in fig. 5.18 by taking the carrier power constant and all the interferers with the same power. If the interference power is reduced by 30 dB, the CIR increases by 9.3 dB.

To combat multipath propagation with significant angular spread (several degrees) in mobile communication systems, the algorithm maintains a low side lobe level for minimum beamwidth, realizable current ratios and fast convergence. Thus, by reducing interference the capacity improvement in WCDMA systems can be achieved by implementing this algorithm.

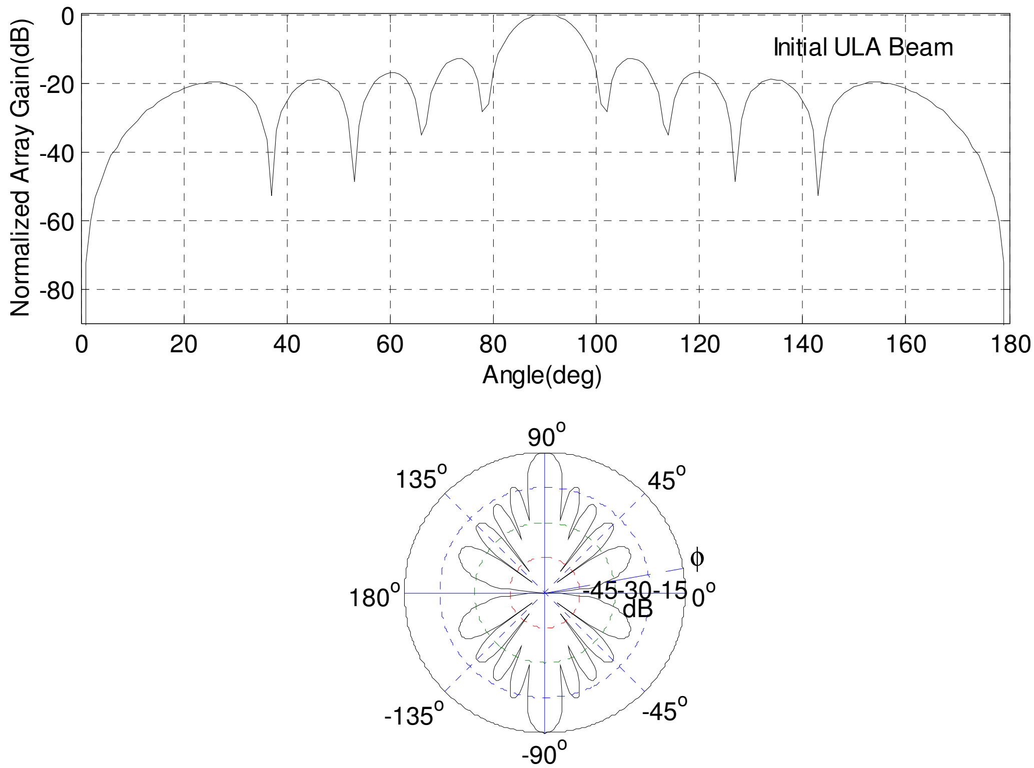

Figure 5.3: ULA pattern for N=10, d=λ/2, $\alpha = 0$

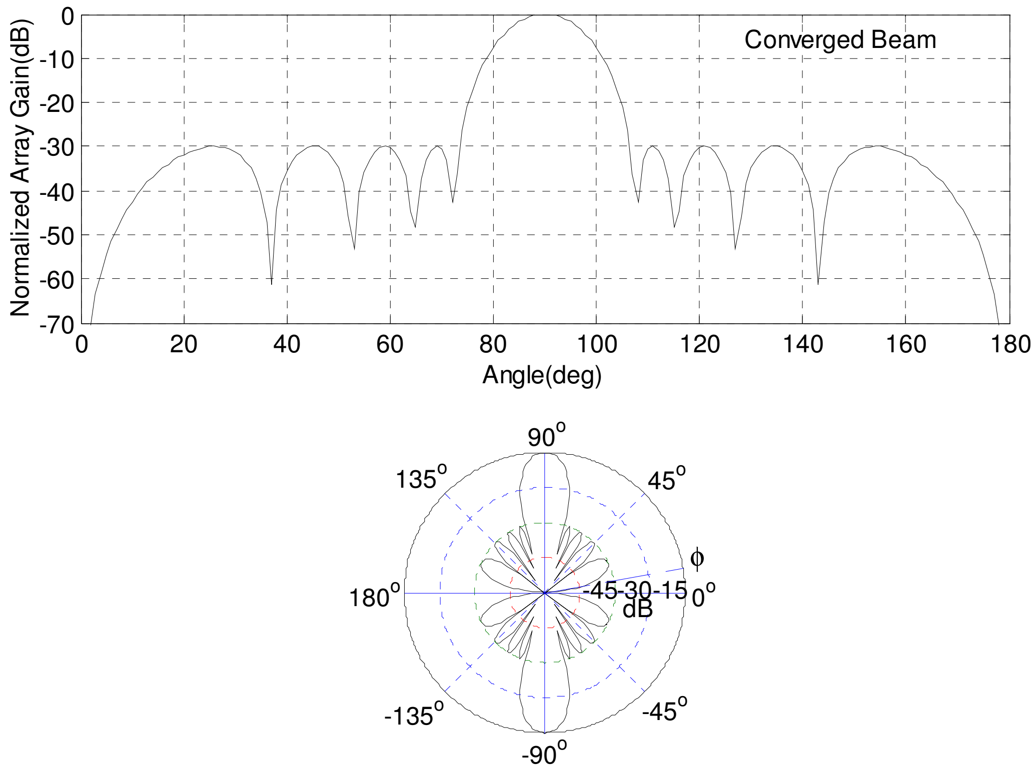

Figure 5.4: Converged Beam for equal sidelobe level of –30 dB; N=10, d=$\lambda/2, \alpha = 0$

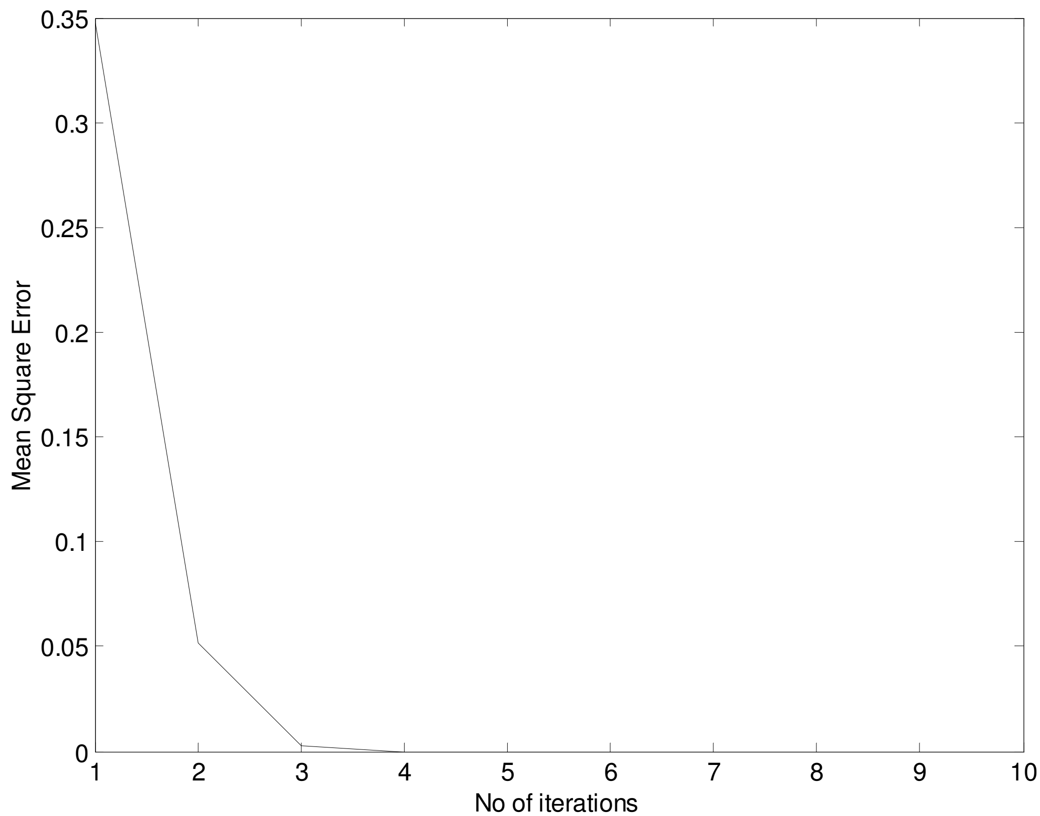

Figure 5.5: Error Graph showing the convergence for N=10

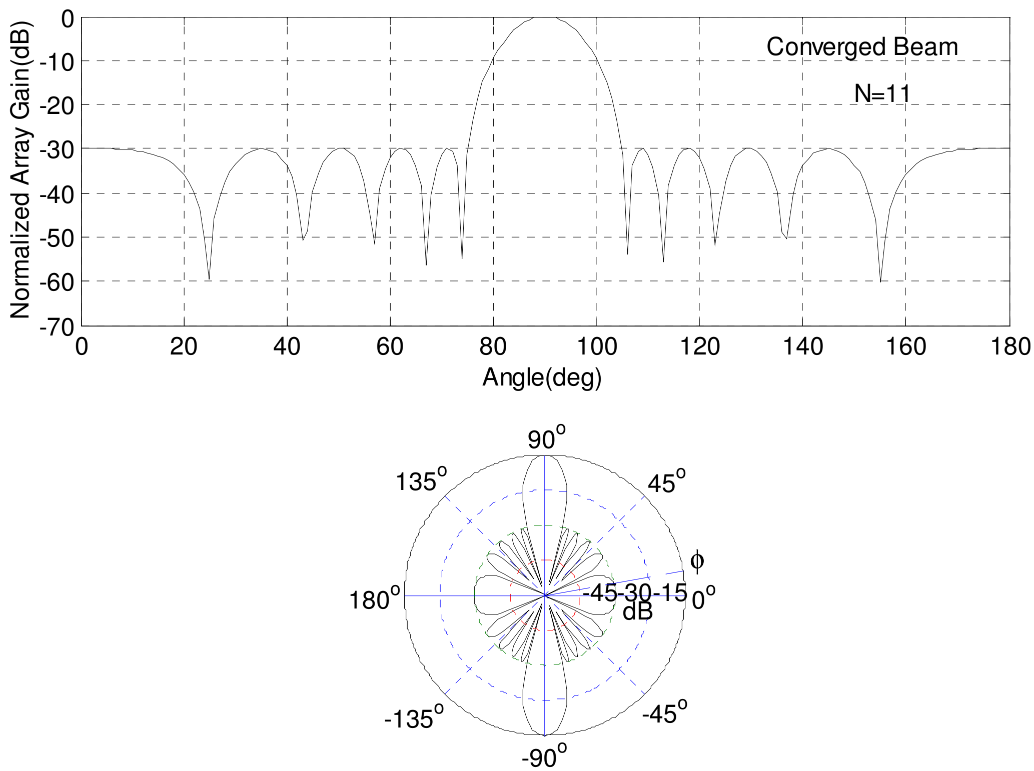

Figure 5.6: Converged Beam for equal sidelobe level of –30 dB; N=11, d=$\lambda/2, \alpha = 0$

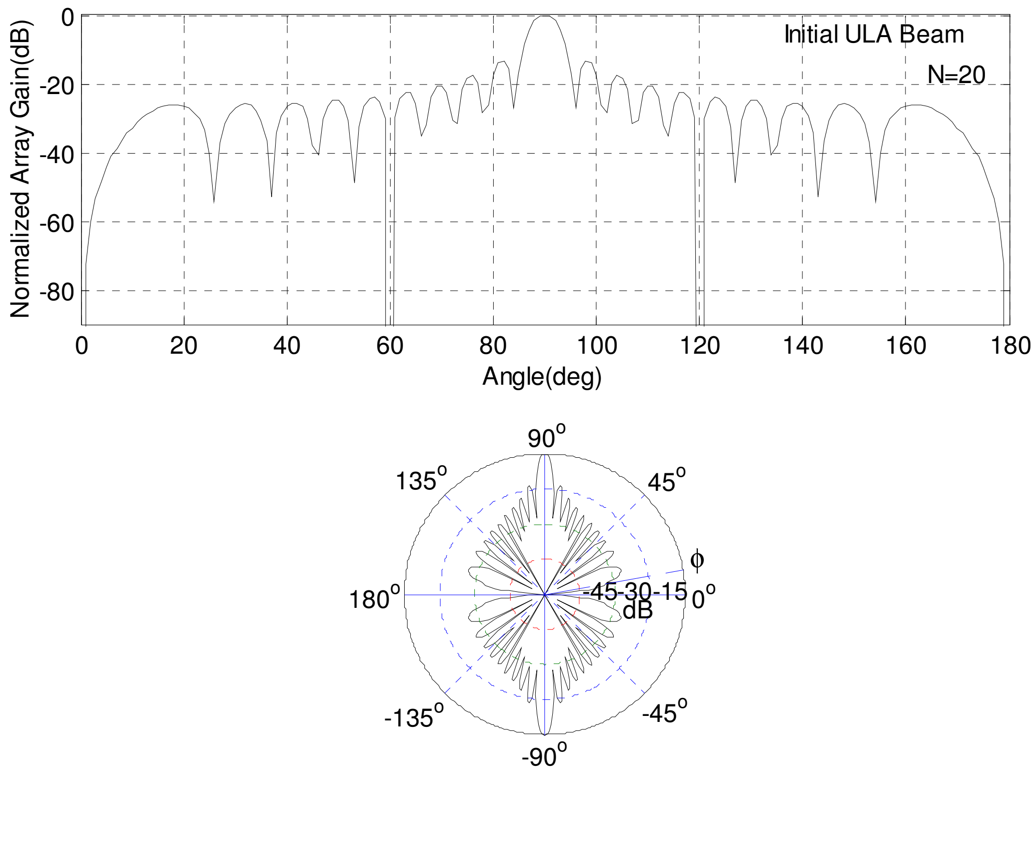

Figure 5.7: ULA Pattern for N=20, d=$\lambda/2, \alpha = 0$

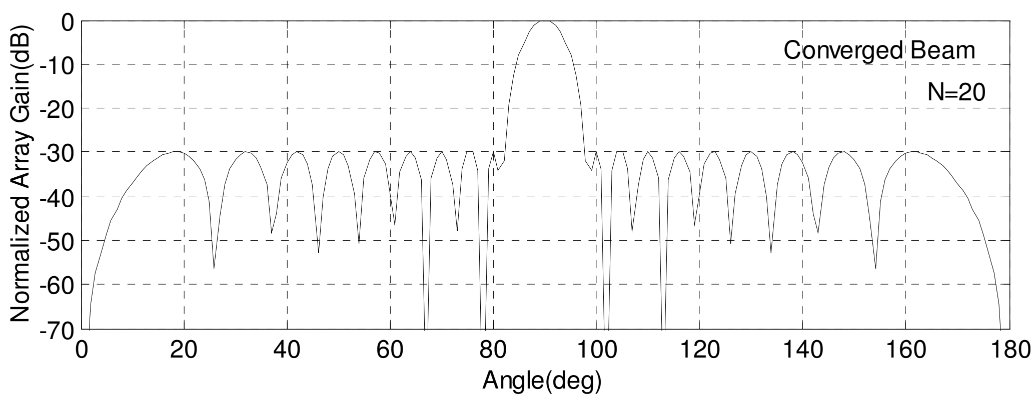
Converged Beam
N=20
Normalized Array Gain(dB)
Angle(deg)
0
-10
-20
-30
-40
-50
-60
-70
0
20
40
60
80
100
120
140
160
180

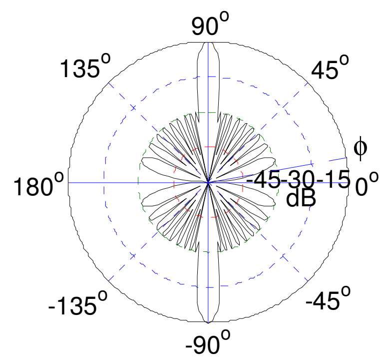
90°
45°
135°
180°
0°
-45°
-135°
-90°
ϕ
-45-30-15
dB

Figure 5.8: Converged Beam for equal sidelobe level of –30 dB; N=20, d=$\lambda/2, \alpha = 0$

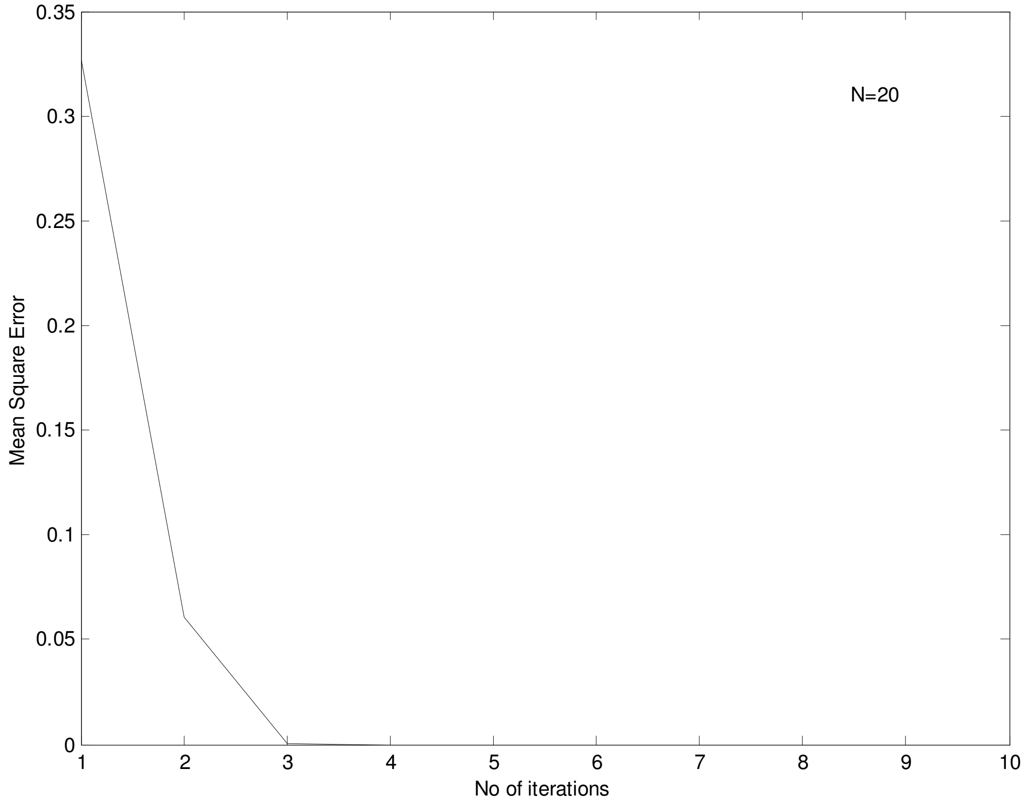

Figure 5.9: Error Graph showing the convergence for N=20

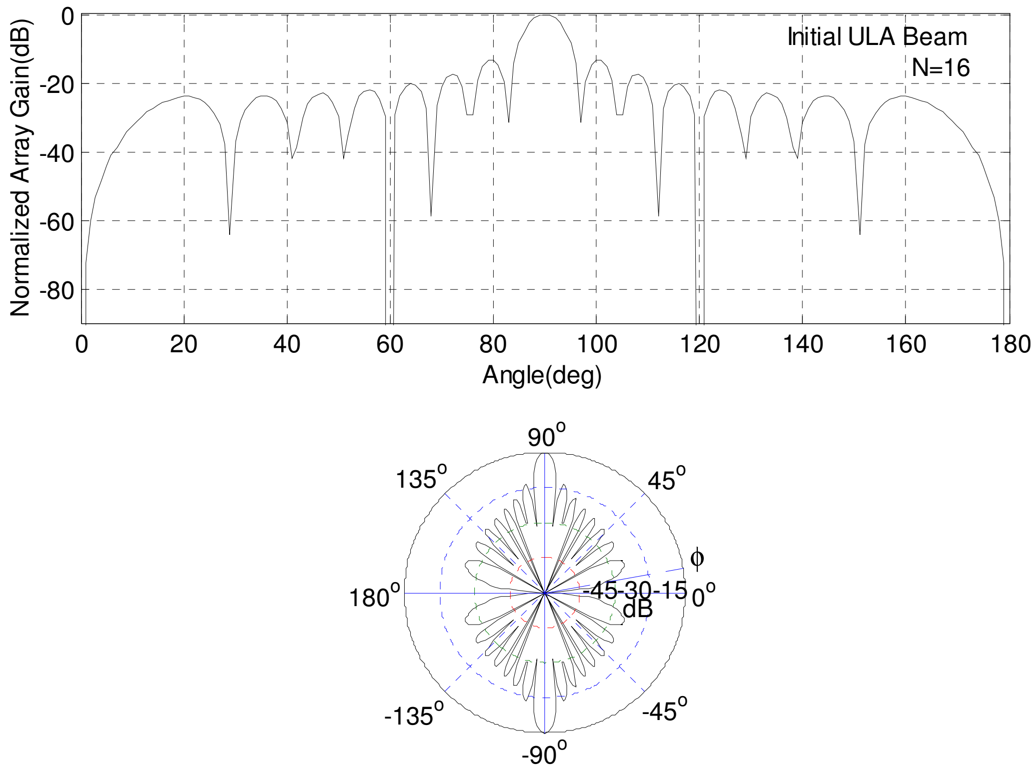

Figure 5.10: ULA pattern for N=16, d=$\lambda/2, \alpha = 0$

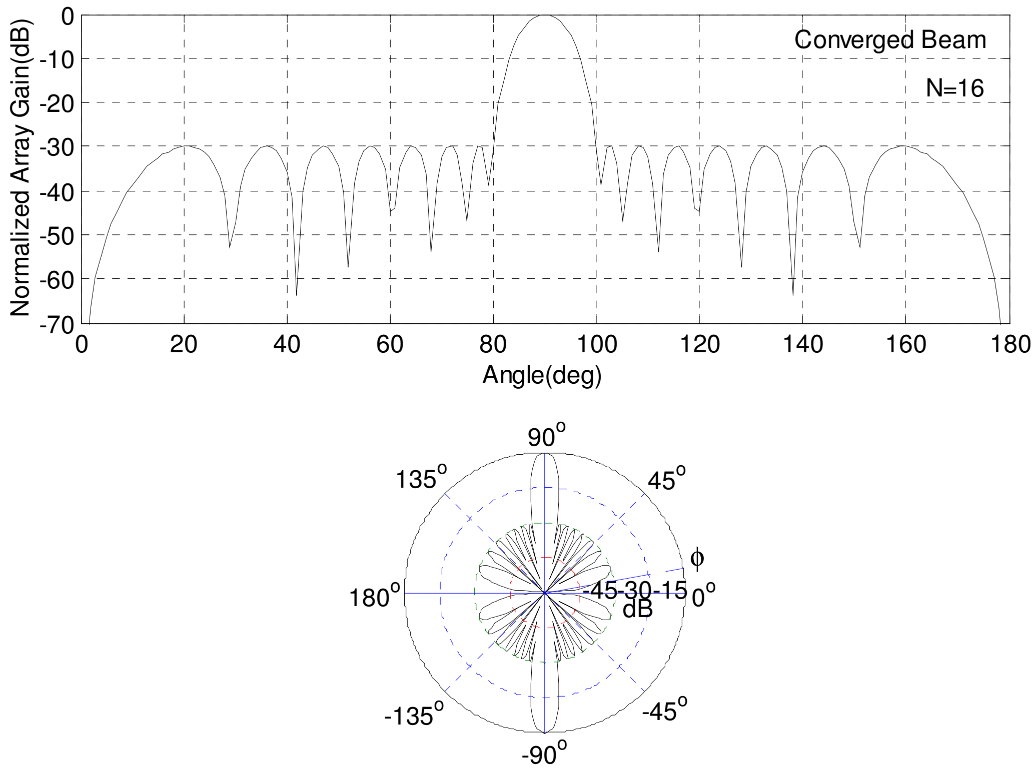

Figure 5.11: Converged Beam for equal sidelobe level of –30 dB; N=16, d=$\lambda/2, \alpha = 0$

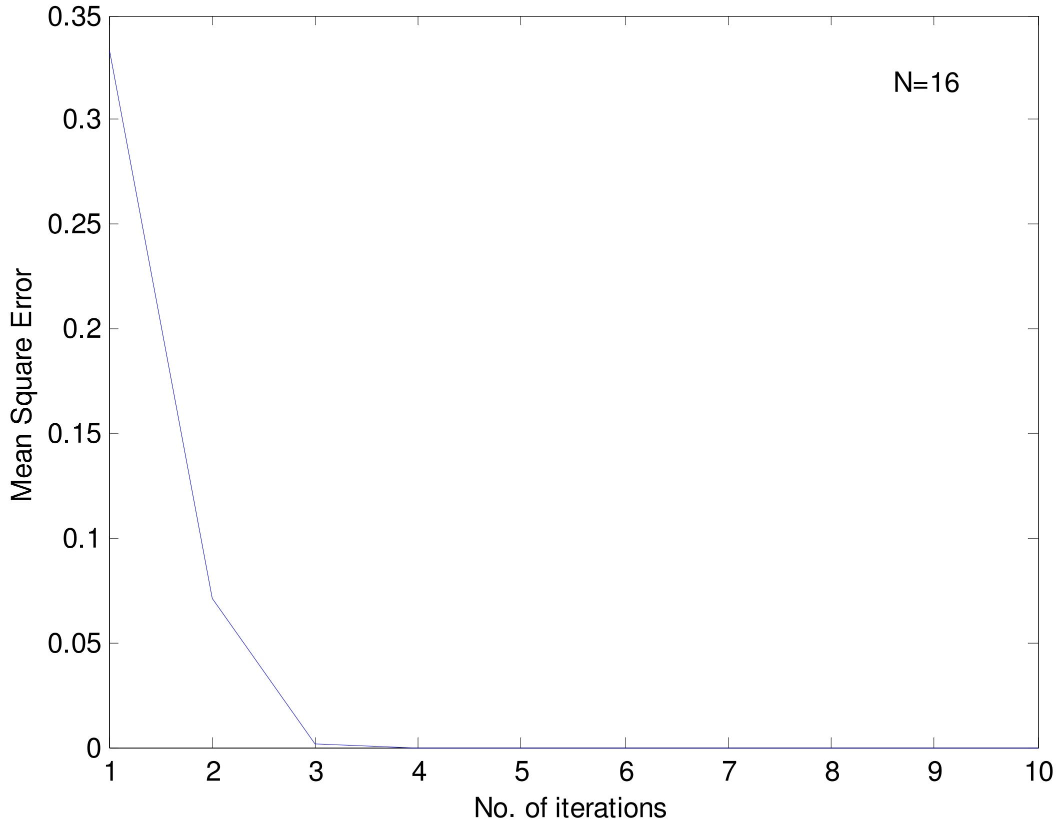

Figure 5.12:Error Graph showing the convergence for N=16

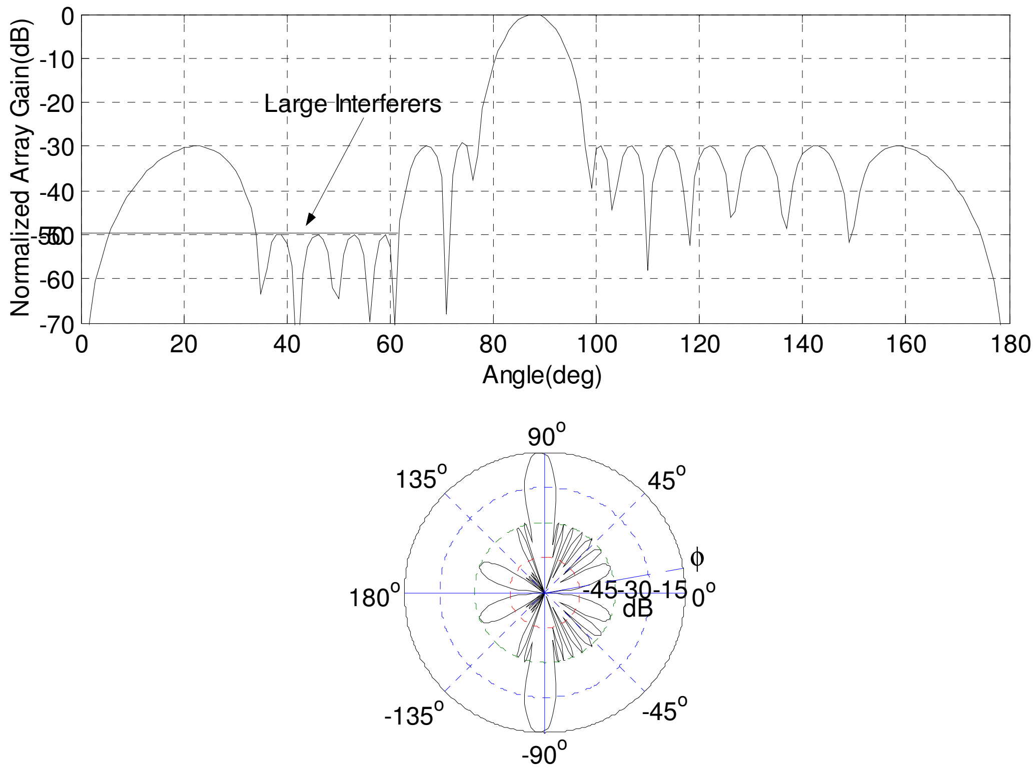

Figure 5.13: Beamforming with grooved-SLT(left) for $N=16, d=\lambda/2, \alpha=0$

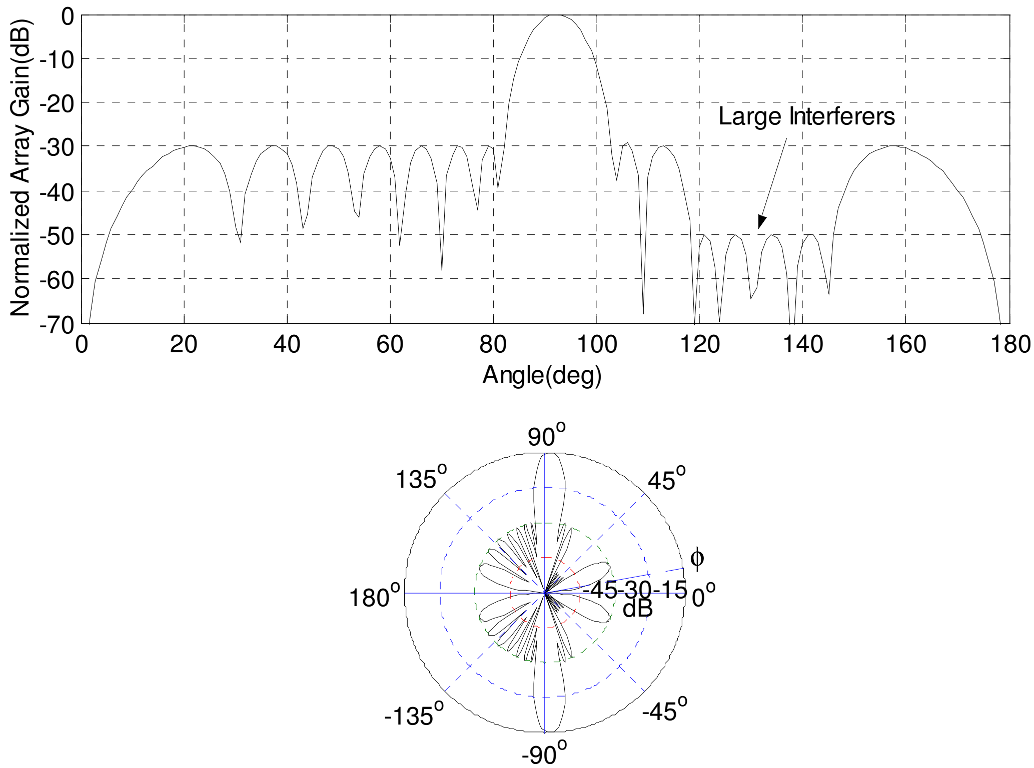

Figure 5.14: Beamforming with grooved-SLT(right) for N=16,d=λ/2,α=0

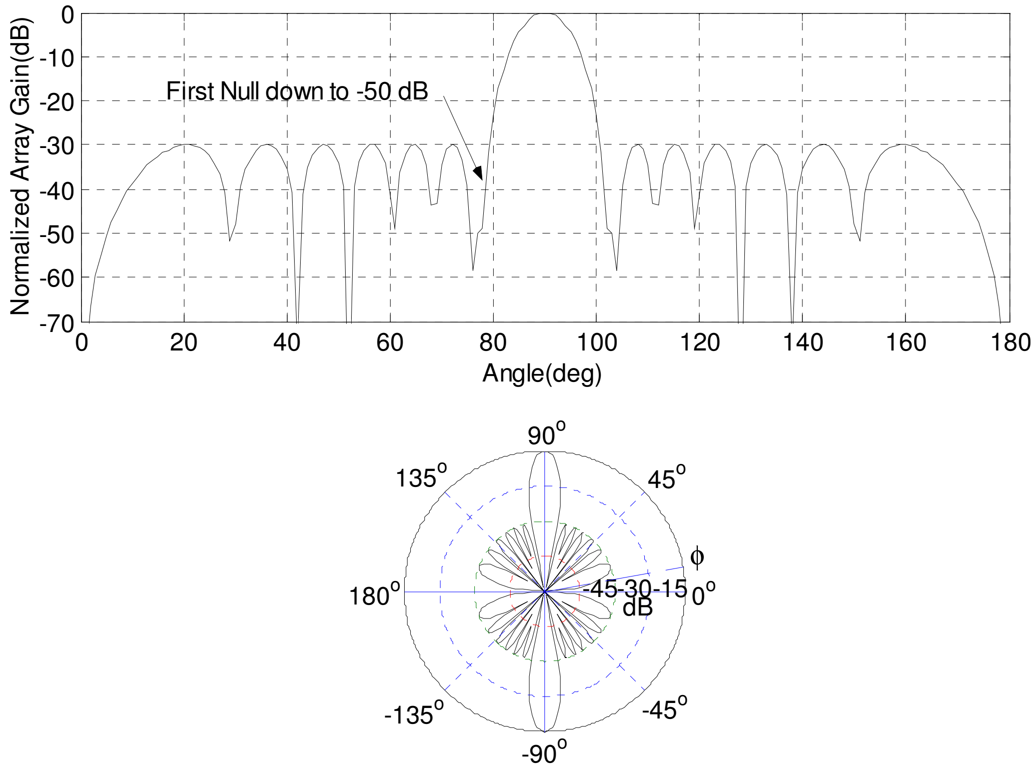

Figure 5.15: Beamforming with inward taper-SLT for N=16,d=λ/2,α=0

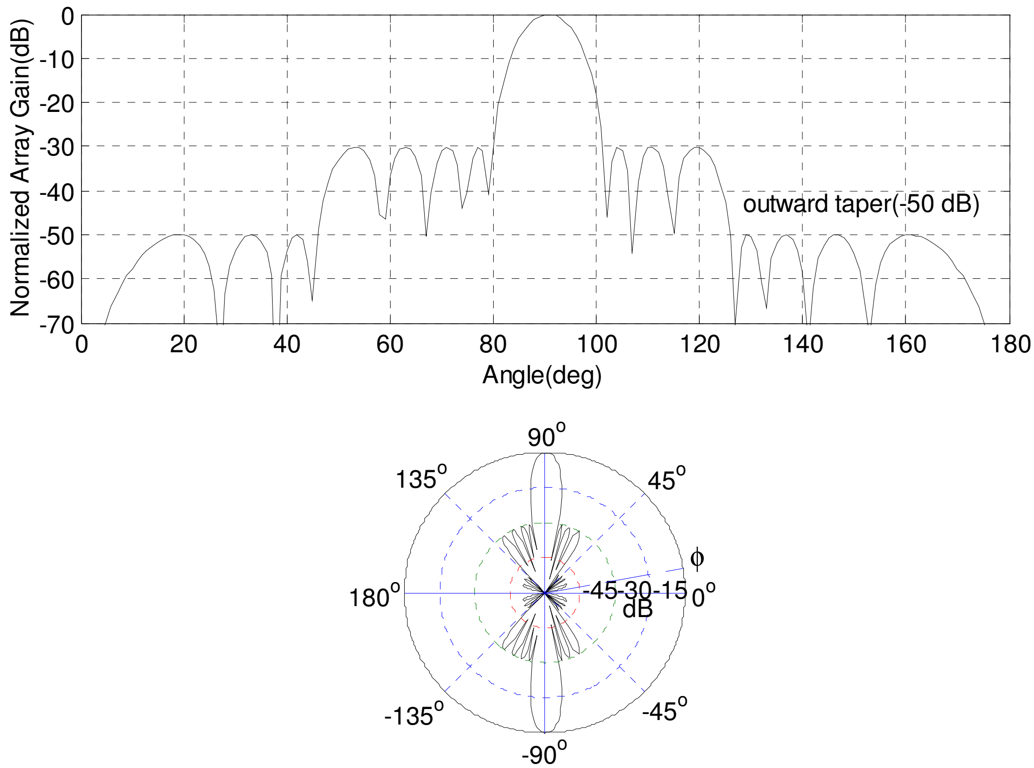

Figure 5.16: Beamforming with outward-taper SLT for N=16,d=λ/2,α=0

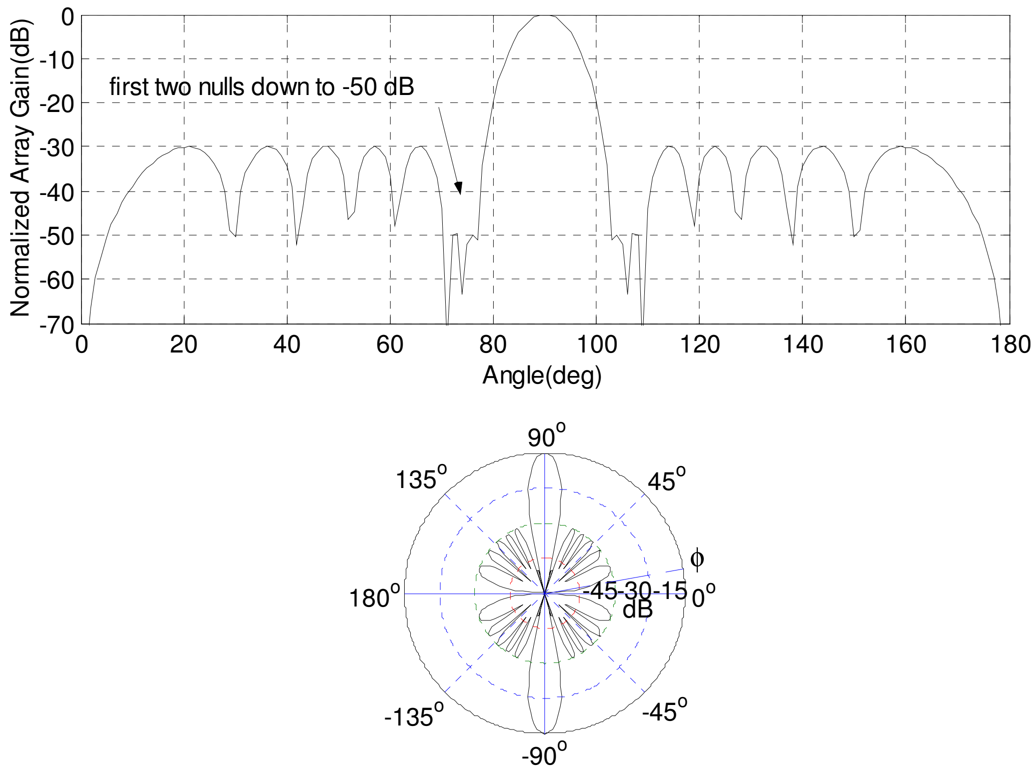

Figure 5.17: Beamforming with inward-taper SLT for N=16,d=λ/2,α=0

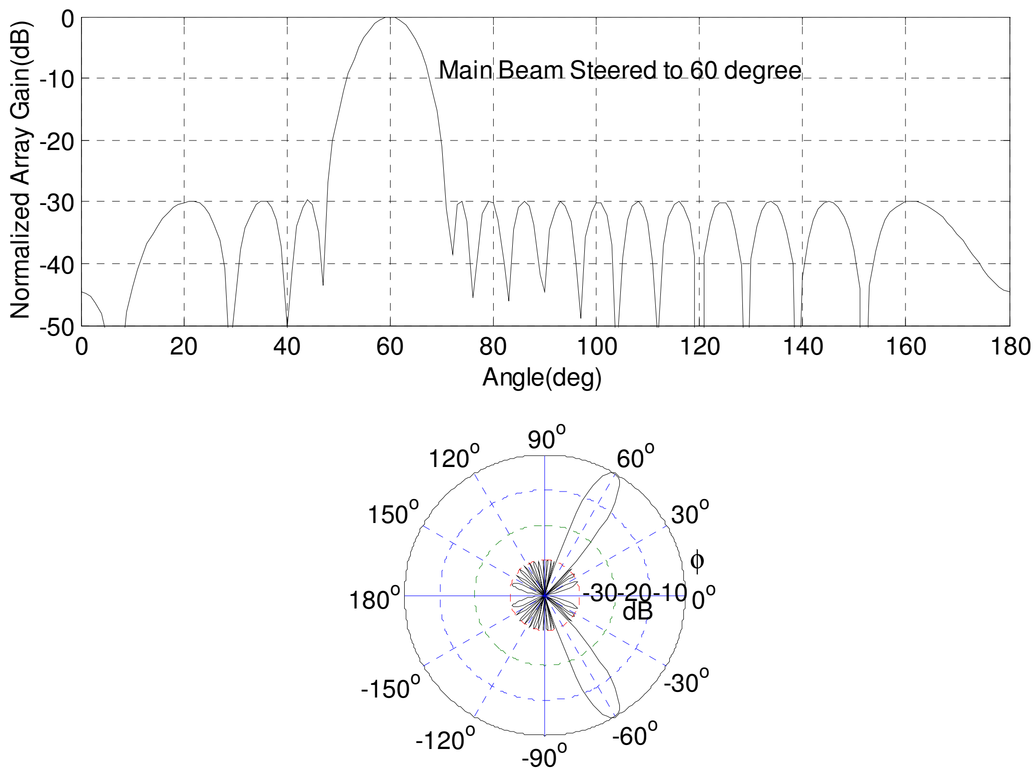

Figure 5.18: Conservation of ESLL property after beamforming, N=16, $d=\lambda/2$, for $\Phi=60^{o}$, $\alpha=0$

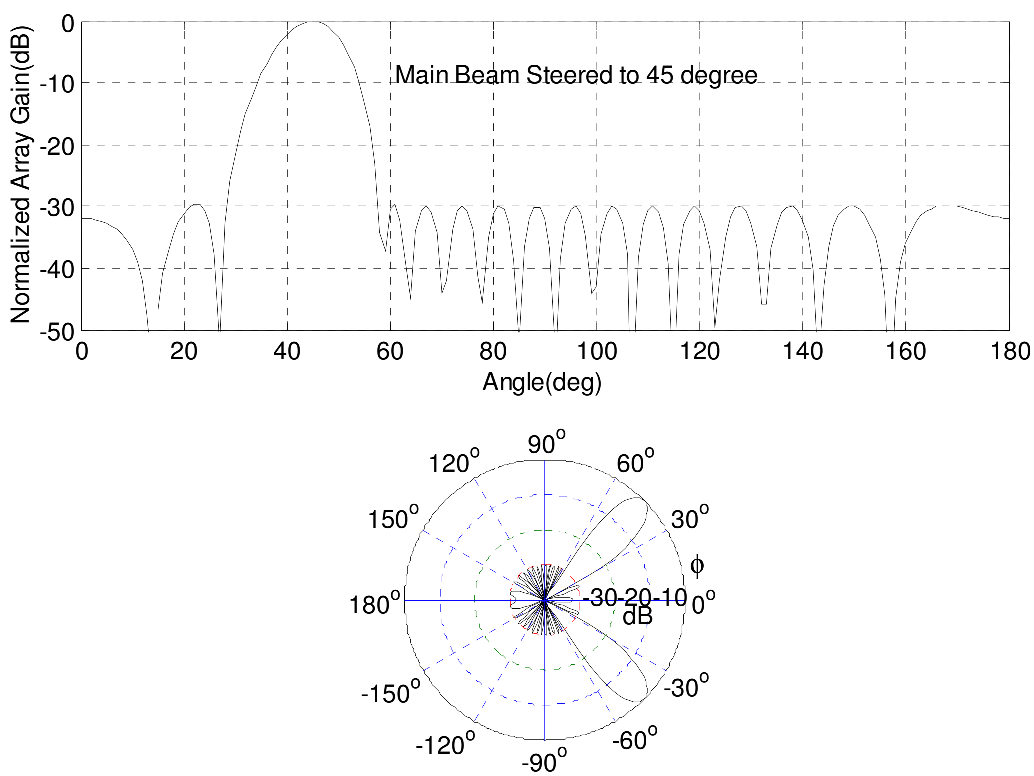

Figure 5.19: Conservation of ESLL property after beamforming, N=16, d=λ/2, for Φ=45°,α=0

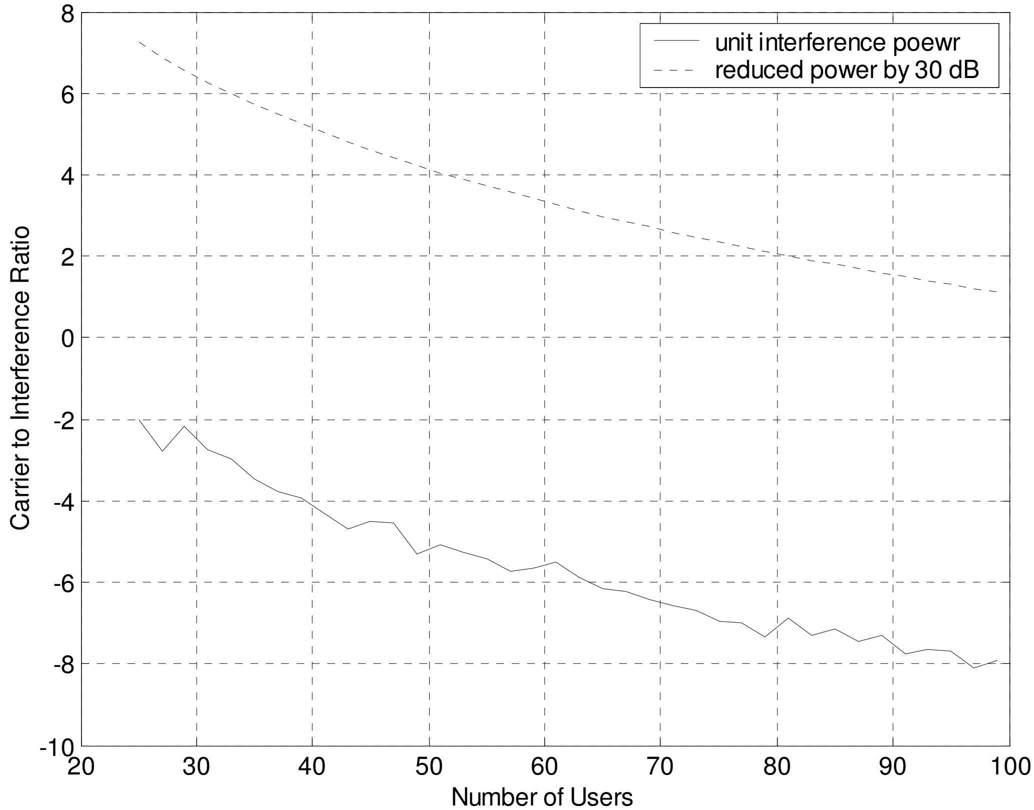

Figure 5.20: Effect of reducing the interference power on the C/I ratio

Chapter 6

Conclusions & Future Scope

There are different beamforming techniques existing today at the antenna array to be used as a transmitter or receiver. In chapter 3 and chapter 4, various non- adaptive and adaptive beamforming techniques for interference cancellation have been discussed. These techniques are based on the same optimality criterion and the optimal weights are given by wiener solution. Antenna arrays using beamforming techniques can reject interfering signals having a direction of arrival different from that of a desired signal. These capabilities can be exploited to improve the capacity of wireless communication systems. There are limitations of earlier adaptive beamforming methods like fixed nulls can be formed, the slow convergence rate, and the computational complexity.

Now in the interferer diversity systems like 3G CDMA systems, as the number of interferers is very large, a new beamforming solution, which can reduce the interference power in a specific direction instead of nulling the individual interferers, would be required. In chapter 5, a new array pattern synthesis procedure is analyzed in which weights are calculated iteratively, till the power ratio assigned to the sidelobes is achieved. This technique has the flexibility of synthesizing any antenna array pattern and deviate from that in case of requirement. The major advantage of this procedure is its simplicity and robustness in adapting to the need. Mostly, equally spaced arrays are used for the transmitter requiring variable array pattern, but this synthesis procedure can be used with non-isotropic elements with arbitrary spacing. In future this can be employed in different array configuration to increase the capacity to a large extent.

References

[1] C.A. Balanis, "Antenna Theory - Analysis And Design", Harper and Row Publishers, New York, 2nd ed., 1997

[2] D.E. Dudgeon, " Fundamentals of digital array processing", Proceeding of the IEEE, vol.65, no.6, pp.98-104, June 1977.

[3] D. G. Manolakis, V. K. Ingle, and S. M. Kogon, Statistical & Adaptive Signal Processing , Tata Mc-Graw Hill, 1st ed., 2000.

[4] E.C. Jordan and K.G. Balmain, "Electromagnetic Waves and Radiating Systems", Second Edition, Prentice Hall of India, New Delhi, 1995.

[5] H. Steyskal, R.A. Shore, and R.L. Haupt, "Methods for Null Control and Their Effects on the Radiation Pattern", IEEE Trans. on Antennas and Propagation, vol. AP-34, no. 3, March 1986.

[6] J.Choi & G.H.Lee, "A Single Beamformer for Antenna Array CDMA Systems", Elsevier Journal of Signal Processing, vol.81,pp.321-334,2001

[7] J.H.Winters,"Smart Antennas for Wireless Systems", IEEE Personal Communications Magazine, pp. 23-27, February 1998.

[8] J.Litva and T.Kwok-Yeung Lo, " Digital Beamforming in Wireless Communication", John Wiley and Sons, New York, 1996.

[9] J. D. Kraus, and R. J. Marhefka, "Antenna for all Applications", Tata McGraw-Hill, 3rd ed., 2002.

[10] J.H.Winters, "Optimum Combining in Digital Mobile Radio with Cochannel Interference", IEEE Trans. on Veh. Tech., vol. 33, pp. 144-155, Aug. 1984.

[11] L.M.Tuan, J.Park, G.Yoon & J.Kim, "Novel LMS based Exponential Step Size Beamforming Algorithm for Smart Antenna" , IEICE Transaction on Communications, vol.E85-B, no.5, May 2002.

[12] L.C. Godara, “ Application of Antenna Arrays to Mobile Communications, Part II: Beamforming and Direction of Arrival Considerations”, Proceedings of the IEEE, vol. 85, 1997.

[13] M. Haardt & Q.Spencer, “Smart Antennas for Wireless Communications beyond the Third Generation”, Elsevier Journal of Computer Communications, no.26, pp. 41–45, 2003.

[14] Ph.D. Thesis on “System Level Improvements in Downlink of TD-CDMA Mobile Communications”, IISC Bangalore, 2001.

[15] P.Petrus, and J.H.Reed, “Capacity Enhancement using Adaptive Arrays in an AMPS System”, IEEE Transactions on Veh.Tech., vol. 47,August 1999.

[16] R.Prasad, “Wideband CDMA for Third Generation Mobile Communication”, Artech House, 1998, pp. 201-218.

[17] S. Choi & D.Shim, “A Novel Adaptive Beamforming Algorithm for a Smart Antenna in a CDMA Mobile Communication Environment”, IEEE transaction on Veh.Tech, vol.49,no.5, pp.1793-1806, September 2001.

[18] T.S Rappaport, “Smart Antennas Adaptive Arrays, Algorithms, and Wireless Position Location”, Published by the IEEE, 1998.

[19] T.S.Rappaport, “Mobile Communication Principles and Practices”, Prentice Hall of India, 2000.

[20] W.C.Y.Lee, “Mobile Cellular Telecommunication System,” McGraw Hill, New York, 1989.